Modulation of Synaptic Vesicle Pools by Serotonin and the Spatial Organization of Vesicle Pools at the Crayfish Opener Neuromuscular Junction

by

Jessica Bilkey
B.Sc., University of Ottawa, 2010

A Thesis Submitted in Partial Fulfillment
of the Requirements for the Degree of

MASTER OF SCIENCE

in the Department of Biology (Neuroscience)

Supervisory Committee

Modulation of Synaptic Vesicle Pools by Serotonin and the Spatial Organization of Vesicle Pools at the Crayfish Opener Neuromuscular Junction

by

Jessica Bilkey
B.Sc., University of Ottawa, 2010

Supervisory Committee

Dr. Kerry R. Delaney (Department of Biology)
Co- Supervisor

Dr. Patrick C. Nahirney (Division of Medical Sciences)
Co-Supervisor

Dr. Raad Nashmi (Department of Biology)
Departmental Member

Abstract

Supervisory Committee

Dr. Kerry R. Delaney (Department of Biology)
Co- Supervisor

Dr. Patrick C. Nahirney (Division of Medical Sciences)
Co-Supervisor

Dr. Raad Nashmi (Department of Biology)
Departmental Member

The crayfish claw opener neuromuscular junction (NMJ) is a biological model for studying presynaptic neuromodulation by serotonin and synaptic vesicle recycling. Serotonin acts on crayfish axon terminals to increase the release of the neurotransmitter glutamate, but a complete understanding of its mechanisms of action are unknown. In order to sustain enhanced neurotransmission over long periods of time, it was hypothesized that serotonin recruits (activates) a population of previously non-recycling vesicles to become releasable and contribute to neurotransmission. To determine if serotonin activates a distinct population of synaptic vesicles, FM1-43 fluorescence unloading experiments were performed on crayfish excitatory opener axon terminals. These experiments could not resolve a serotonin-activated population of synaptic vesicles, but instead revealed that synaptic vesicles change behaviour in axon terminals independent of serotonin, with vesicles becoming less likely to exocytose and unload FM1-43 dye over time. The change in behaviour was hypothesized to be due to conversion of vesicles from a recycling (releasable) status to a reserve (reluctant to release) status. Synaptic vesicle pool localization was then tested using photoconversion of FM1-43 and transmission electron microscopy techniques. The spatial location of FM1-43-labeled vesicles fixed 2 minutes following 20 Hz stimulation did not reveal retention of vesicles specifically near release sites and the distribution of FM1-43-labeled vesicles was not significantly different between early (2 min) and late (180 min) time points. Terminals fixed 30 seconds following stimulation, however, contained numerous endosome-like structures - the most frequently observed structures resembled large vesicles, which were the equivalent of 2-5 regular vesicle sizes. These results suggest that crayfish axon terminals recycle vast amounts of membrane in response to sustained 20-Hz stimulation and endocytosis appears to occur via multiple routes with the most common being through large vesicle intermediates.

Table of Contents

List of Figures

List of Abbreviations

5-HT	5-Hydroxytryptamine, serotonin
AP	Action potential
AZ	Active zone
$[Ca^{2+}]_i$	Intracellular free calcium concentration
CF	Cationized ferritin
CNS	Central nervous system
DAB	3,3'-Diaminobenzidine
HRP	Horseradish peroxidase
NA	Numerical aperture
RP	Reserve pool
RRP	Readily releasable pool (a.k.a. recycling pool)
TEM	Transmission electron microscopy

Acknowledgments

I would like to thank Dr. Kerry Delaney for his knowledge and generous support, Dr. Patrick Nahirney for his mentorship and thorough editing of my thesis, and both for the opportunity to do my thesis work in their labs. I also thank Dr. Raad Nashmi for his helpful comments and critiques during lab and committee meetings and Dr. Paul Zehr for providing his time as the external examiner. I owe a sincere thank-you to Drs. Adam Fekete and Stuart Trenholm and to David Stuss for their guidance. I am grateful to Jay Leung for his invaluable assistance with TEM analysis and I also thank Geoff DeRosenroll for providing technical support and Sammy Weiser Novak for his TEM contributions.

Without these individuals this work would not have been possible: Karen Myers, Eleanore Blaskovich, David McPhee and past members of the Delaney lab, Anthony Renda, Pragya Komal, Angela Seto and fellow Neuroscience trainees, and the Outdoor Aquatic Unit staff.

I am so grateful for the love and support from Teio, Carolyn, Dave, Lindsay and Mckenzie.

Dedication

To the three amigos.

Chapter 1 – Introduction

The foundation of neuronal signalling is electro-chemical transmission. Fast chemical transmission between neurons and target cells occur at sites called synapses, with delays of less than a millisecond (Borst and Sakmann, 1996; Sabatini and Regehr, 1996). At fast transmitting synapses, neurotransmitters are stored in small vesicles in the presynaptic axon terminal (reviewed by Jahn and Südhof, 1994). Release of neurotransmitter is stimulated by a brief influx of Ca^{2+} ions through voltage-gated calcium channels in response to action potentials (APs) (reviewed by Catterall and Few, 2008). Released neurotransmitters diffuse rapidly across the synaptic cleft and bind to postsynaptic receptors that gate ion channels, causing a change in the postsynaptic membrane potential.

Release of transmitter-containing synaptic vesicles occurs at specialized sites called active zones. Active zones contain the protein scaffolding required to dock, prime, and fuse synaptic vesicles with the presynaptic membrane in a process known as exocytosis (reviewed by Jahn and Südhof, 1994). After the release of neurotransmitter, some form of retrieval takes place (endocytosis) to recover a roughly equivalent amount of fused vesicle membrane and the vesicle-associated proteins (Heuser and Reese, 1973; Sun et al., 2002; Watanabe et al., 2013a,b). The process of exocytosis and endocytosis is known as 'recycling'.

The regulation and modification of neurotransmitter release is the basis of chemical synaptic transmission. The efficacy of synapses is finely regulated and enables response to changing circumstances and the demands of the system. Regulation of synaptic transmission can occur via activity-dependent or modulator-mediated processes. Serotonin (5-hydroxytryptamine or 5-HT) is a biogenic amine found in vertebrates, invertebrates and plants (Azmitia, 2001) and is a potent modulator of neurons and other tissues in vertebrates (Bunin and Wightman, 1999) and invertebrates (Dixon and Atwood, 1985, 1989a,b; Dudel, 1965; Glusman and Kravitz, 1982). At invertebrate synapses, such

as the neuromuscular junctions (NMJs) of crustacea, serotonin increases the release of neurotransmitter-containing synaptic vesicles (Dudel, 1965). Crustacean NMJs are simple and similar to vertebrate central synapses and therefore are popular models for investigating modulation by serotonin. The mechanisms by which serotonin modulates synaptic transmission continue to be studied and is a theme of this thesis.

1.1 Crustacean neuromuscular junctions as synapse models

Crustacean NMJs, including those of lobster, crab and crayfish, have been used for decades to investigate properties of synaptic transmission (Cooper et al., 1995; Cooper et al., 1996; Dudel and Kuffler, 1961a; Govind and Meiss, 1979; Wojtowicz et al., 1991; Wojtowicz et al., 1994) and modulation of synaptic transmission (Delaney et al. 1991; Dudel, 1965; Fischer and Florey, 1983). The dissections are simple and preparations can be kept alive and healthy with minimal effort for several hours and so are ideal for long experiments. The systems also provide *ex vivo* investigation of synapses without complicated interactions from a network of dense cells, as is the case with vertebrate central nervous systems (CNS).

The discrete nature of crustacean axon terminals make them suitable for techniques involving live fluorescence imaging, including vesicle labeling with styryl dyes like FM1-43 (Wang and Zucker, 1998). Crustacean NMJs are also useful for studies comparing physiological and ultrastructural data because single terminals can be tracked and visualized with electron microscopy (Johnstone et al., 2011). Crustacean studies continue to address the presynaptic mechanisms underlying modulation of transmitter release, regulation of synaptic vesicle pools, and other fundamentals of synaptic transmission, with experiments mainly conducted on the crayfish *Procambarus clarkii* (Pan and Zucker, 2009; Wang and Zucker, 1998; Wu and Cooper, 2012).

1.1.1 Crayfish NMJs are similar to vertebrate central synapses

Crayfish NMJs are valuable models for synaptic physiology because of their similarity to vertebrate central synapses. Crayfish motor neurons release the neurotransmitters glutamate and GABA (γ-aminobutyric acid) (Bazemore et al., 1957; Kerkut et al., 1965; Robbins, 1959), identical to the main excitatory and inhibitory neurotransmitters in the vertebrate CNS. The structural and biochemical properties of the cellular machinery that produce transmitter release are also highly conserved (reviewed by Zhai and Bellen, 2004), as are synaptic vesicle-associated proteins (Cooper et al., 1995), presynaptic voltage-gated calcium channels (Hong and Lnenicka, 1997) and metabotropic receptors (Tabor and Cooper, 2002).

Crayfish NMJs demonstrate similar phenomena to vertebrate central synapses including short- and long-term activity dependent enhancement of transmitter release (Dudel and Kuffler, 1961b; Sherman and Atwood, 1972), presynaptic inhibition (DeMill and Delaney, 2005; Dudel and Kuffler 1961c), synaptic differentiation (Bittner, 1968; Cooper et al., 1995) and modulation of transmitter release by biogenic amines like serotonin (Delaney et al., 1991; Dudel, 1965; Vyshedskiy et al., 1998; Wang and Zucker, 1998). Studying the fundamentals of synaptic physiology in relatively simplistic synapse models such as crayfish NMJs provides a basis for information gathering that can also be applied or compared to higher systems like the vertebrate CNS.

1.2 Modulation of crustacean physiology and behaviour by serotonin

Serotonin acts as a circulating neurohormone in crustaceans (Evans et al., 1976; Livingstone et al., 1981). It is released into the hemolymph from pericardial organs and by nerve endings in thoracic roots (Beltz and Kravitz, 1983). Crustaceans have an open circulatory system so serotonin released into the hemolymph will bathe a multitude of organs including neuromuscular junctions of skeletal muscle. General physiological effects of serotonin include increasing heart rate (Listerman et al., 2000) and acting on

discrete circuits that control movements of the foregut (Ayali and Harris-Warrick, 1999). Serotonin also regulates escape behaviours (Yeh et al., 1996), decreases locomotion (Tierney and Mangiamele, 2001; Tierney et al., 2004) and produces characteristic 'serotonin postures' (Harris-Warrick and Kravitz, 1984; Livingstone et al., 1980; Tierney and Mangiamele, 2001). One example of a serotonin posture is “high posture” where the animal holds an elevated stance above the substrate with its abdomen flexed under its body (Tierney and Mangiamele, 2001). The behavioural significance of the postures induced by serotonin in crayfish is not understood but they do not appear to be aggressive, as previously thought (Tierney and Mangiamele, 2001). Overall serotonin has multiple effects on crustacean physiology and behaviour depending on the target organs and the concentration of the modulator in the hemolymph.

1.2.1 Serotonin increases neurotransmission at crustacean synapses

Serotonin acts on crustacean NMJs to modulate the release of neurotransmitter-containing synaptic vesicles. Early intracellular recordings of postsynaptic membrane potentials determined that low concentrations of serotonin increased spontaneous and AP-evoked vesicle release (Dudel, 1965), indicating a presynaptic action of the modulator. The enhancement of synaptic transmission in response to 5-minute application of serotonin can last for up to an hour (Dixon and Atwood, 1985). The mechanism of action of serotonin at presynaptic axon terminals is not well understood, however. At the crayfish opener NMJ, serotonin binds to putative 5-HT_2-like receptors on the presynaptic membrane (Tabor and Cooper, 2002) and activates at least two second messenger systems involving adenylate cyclase and phosphatidylinositol (Dixon and Atwood, 1989a,b). The targets of the messenger systems are mostly unknown, but one hypothesis is that activation of phospholipase C leads to production of 1,4,5-triphosphate (IP_3) and release of Ca^{2+} from internal stores (Wu and Cooper, 2012). Experiments using fura-2 imaging, however, revealed that serotonin does not cause significant increases in resting presynaptic calcium ($[Ca^{2+}]_i$), nor AP-mediated Ca^{2+} influx (Delaney et al., 1991). Importantly, the authors observed that small increases in $[Ca^{2+}]_i$ by serotonin did not persist once the modulator was removed. Delaney et al. (1991) also determined that local

undetectable increases in $[Ca^{2+}]_i$ (released from intracellular stores) likely do not underlie serotonin's effects because intracellular injection of the calcium buffer EGTA did not diminish enhancement of the EJPs. The authors discussed the possibility of IP_3-mediated release of calcium from internal stores in the axon terminals, but concluded that the resulting calcium concentration would be neither sufficient to overcome the buffering capacity of the terminal nor necessary for enhanced transmitter release.

Since serotonin induced enhancement is not dependent upon changes in presynaptic calcium influx nor increased resting $[Ca^{2+}]_i$ it could enhance neurotransmission by directly modulating the release machinery at active zones, possibly leading to more release competent sites for vesicle fusion (as discussed by Delaney et al., 1991). This idea is supported by the behaviour of crayfish NMJs in response to repetitive stimulation in the absence and presence of serotonin. Crayfish NMJs have low vesicle release probabilities but demonstrate marked enhancement of EJPs (e.g. 10-100 fold) in response to repetitive stimulation. When serotonin is present, the amount of neurotransmitter released (mean quantal content) is increased for each stimulus, but the amount of facilitation is not changed from non-serotonin conditions (Sparks and Cooper, 2004). There is also a notable drop in the coefficient of variation (CV) resulting from both an increase in the mean EJP amplitudes and a decrease in the variation of the EJP amplitudes. This implies that serotonin increases the probability of vesicle fusion and allows for the fusion of more vesicles per stimulus delivered. The increased probability of vesicle release could be the result of serotonin recruiting more active zones, or serotonin adding more release competent sites to existing active zones, or serotonin increasing the likelihood of vesicle exocytosis at existing release sites within existing active zones. Recruitment of active zones by serotonin was investigated using FM1-43 and FM4-64 dye imaging techniques but the results showed no obvious increases in the number of active zones (Wang and Zucker, 1998). Additional experiments in the same study used an analysis of synaptic depression and labeling of recycling vesicles with FM1-43 to reveal that serotonin increased the pool size of recycling (releasable) vesicles (Wang and Zucker, 1998). An enhancement of the recycling pool would result in increased probability of fusion of any of the recycling vesicles. Whether serotonin

modifies existing active zones to add more release sites remains to be determined and the mechanism behind the observed increase in the number of recycling vesicles is also unknown. A central theme of Chapter 3 in this thesis was to verify whether serotonin increases the number of recycling synaptic vesicles in order to explore potential mechanisms.

1.3 Synaptic vesicle pools

Within presynaptic axon terminals, a small percentage of synaptic vesicles are found docked at specialized release sites on the presynaptic membrane, while the remainder reside in an adjoining cluster (reviewed by Rizzoli and Betz, 2005). Although synaptic vesicles look identical under the electron microscope, they are not all functionally equivalent and the classification of vesicles into functionally distinct pools has become widely accepted in almost all model synaptic preparations, including NMJs of frog and *Drosophila*, cultured hippocampal synapses, the mammalian Calyx of Held and goldfish retinal bipolar cells (reviewed by Rizzoli and Betz, 2005). The main functional vesicle pools are typically referred to as "readily releasable", "recycling", and "reserve" pools but they have been called by other names. The recycling pool contains vesicles that recycle during physiological conditions and the readily releasable pool (RRP) consists of the recycling vesicles that are physically docked at release sites. These two functional pools are often grouped together, and will be collectively referred to as the recycling pool in this thesis. The reserve pool (RP) hosts the vesicles reluctant to release and which are, therefore, only recruited after depletion of the recycling vesicles or in high demand situations (reviewed by Denker and Rizzoli, 2010).

1.3.1 Synaptic vesicle pools: mobility and maintenance of identity over time

Recent investigations have focused on characterizing functional vesicle pools, specifically in terms of mobility and maintenance of identity. It was originally assumed

that synaptic vesicle pools were mostly stable at rest and did not become mobile until a stimulus was delivered. The previous assumption also held that vesicles would move toward release sites upon stimulation. However, more recent studies have shown that recycling vesicles are actually mobile at rest whereas reserve vesicles are comparatively immobile, as determined by fluorescence recovery after photobleaching (FRAP) experiments in frog NMJs (Gaffield et al., 2006). Synaptic vesicle movements have also been monitored in cultured hippocampal neurons using stimulated emission depletion (STED) microscopy, which allows for high resolution tracking of single vesicles (Westphal et al., 2008). The Westphal et al. (2008) study found that recycling vesicles are mobile and move both diffusively within axon terminals and directionally by active transport between axon terminals. Synaptic vesicles can also become temporarily fixed in 'hot spots' of axon terminals (Westphal et al., 2008). These spots are assumed to be pockets within the main synaptic vesicle clusters. In contrast to mobile recycling vesicles, reserve vesicles remain immobile until activated by high frequency stimulation (Gaffield et al., 2006). The immobility of reserve vesicles is thought to be due to soluble protein tethers like synapsin (reviewed by Cesca et al., 2010) that associate with lipid and protein components of synaptic vesicles in a phosphorylation-dependent manner (Benfenati et al., 1989; Ceccaldi et al., 1995; Hosaka et al., 1999). Based on these studies it is hypothesized that synapsin molecules bind synaptic vesicles into large clusters and prevent them from freeing until high activity causes them to phosphorylate and dissociate from the vesicles, giving them mobility.

As with vesicle mobility, assumptions regarding vesicle identity have been modified in recent years. Endocytosis of vesicles occurs in regions adjacent to the release sites called peri-active zones (Roos and Kelly, 1999; Teng et al., 1999; Teng and Wilkinson, 2000). Newly formed vesicles classify as recycling because functionally they are mobile and release-competent (Kamin et al., 2010). It has recently been shown that recycling vesicles do not maintain their mobility over time. For example, a study using STED microscopy observed loss of mobility of recycling vesicles over hours in rat cultured hippocampal neurons (Kamin et al., 2010). The authors reported initial mobility of vesicles but a decrease in motion over time as vesicles incorporated into hot spots. The

mobility decreased substantially and led the authors to conclude that mobile recycling vesicles were incorporating into reserve clusters in a process termed “maturation” (Figure 1). The current hypothesis, therefore, is that recycling vesicles will eventually accumulate enough soluble protein tethers that they will adhere to the main vesicle cluster, thereby changing functionality.

Improved higher resolution light microscopy has led to a new understanding of functional vesicle pools with respect to mobility and identity over time. The present understanding is that recycling vesicles are mobile at rest and under normal physiological conditions, displaying both random and directional movements. The reserve vesicles are, in contrast, immobile and tethered to each other in a cluster by soluble vesicle-associated proteins. Recycling vesicles maintain their identities for minutes to hours, but can eventually mature into reserve vesicles as they integrate into the main vesicle cluster. Figure 1 depicts the current understanding of functional vesicle pools.

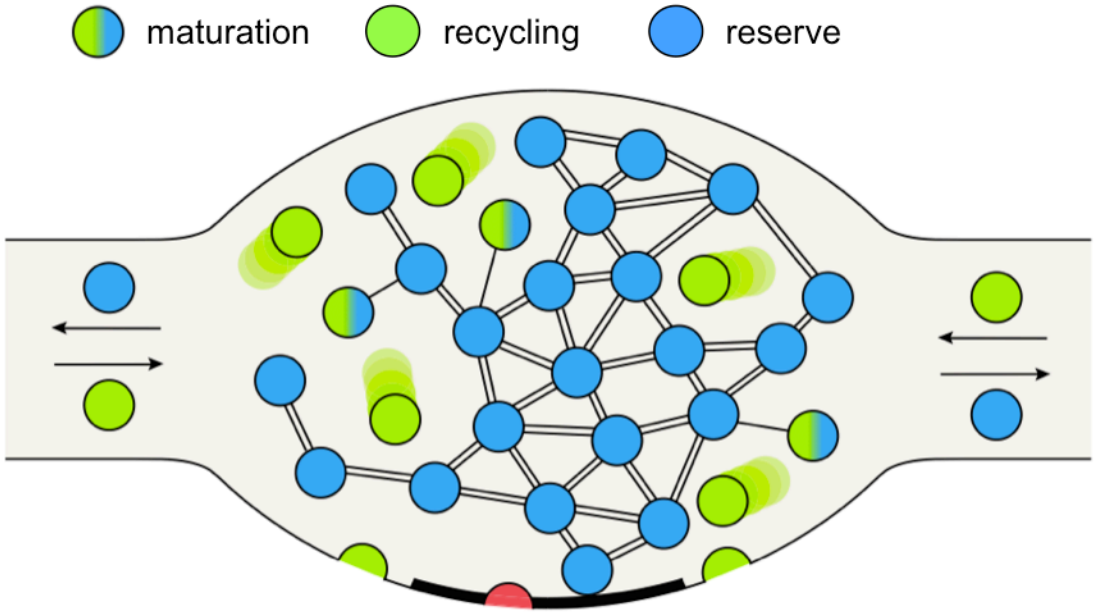

Figure 1. Synaptic vesicle pools. Newly endocytosed recycling vesicles (green) display diffusive movements within axon terminals and directional movements between terminals. The reserve vesicles (blue) are clustered together with soluble vesicle-associated proteins (double bonds) and are predominately immobile unless they are

transporting between axon terminals (Staras et al., 2010). Recycling vesicles can mature and integrate into the reserve cluster over time but their initial association with the reserve cluster is not as tight (single bonds) as the reserve vesicles (double bonds), likely due to fewer protein tethers. The illustration depicts a vesicle fusing (red) at the release site (black band). Modified from (Denker and Rizzoli, 2010).

1.4 Overview and Objectives

In this thesis we first investigated the prediction that serotonin increases the population of recycling vesicles in order to maintain elevated neurotransmitter release (Chapter 3). This was accomplished by utilizing an FM1-43 dye unloading technique, with the intention of further investigating the effects of serotonin. Our initial investigations with serotonin led to a subsequent FM1-43 dye unloading experiment that examined the identities of functional synaptic vesicle pools and vesicle positions within axon terminals over time, independent of serotonin (Chapters 3 and 4). Specifically, we tested the hypothesis that recycling vesicles mature into reserve vesicles over time using FM1-43 photoconversion and electron microscopy. The data from our crayfish NMJ experiments contributes to findings about synaptic vesicle pools and vesicle recycling in other synapse models including the NMJ of frog (Rizzoli and Betz, 2004), *Drosophila* (Denker et al., 2009; Kuromi et al., 2004) and snake (Teng and Wilkinson, 2000), as well as cultured neurons (Harata et al., 2001). The ultrastructural data also contributes to recent novel findings regarding synaptic vesicle endosomes (Schikorski, 2014; Watanabe et al., 2013).

Chapter 2 – General Materials and Methods

2.1 Animals and Preparation

Crayfish (*Procambarus clarkii*, 6-8 cm) were obtained from Atchafalaya Biological Supply (Raceland, LA, USA) and maintained in the aquatic facility at the University of Victoria. They were housed in tanks with filtered, flowing water and maintained at 18°C. Crayfish were provided with PVC tubing for shelter and fed dried fish food. All experiments were performed on the dactylopodite abductor muscle ('opener muscle') in the propodite segment of the first walking leg (Figure 2). The legs were removed from the body at the joint between the basipodite and ischiopodite segments with scissors. The joint between the meropodite and carpopodite segments was then cut with a scalpel to allow for later removal of the meropodite cuticle. To access the opener muscle, the ventral half of the propodite cuticle was cut with a scalpel. The dorsal side of the dactylopodite, propodite and carpopodite segments were then glued to the bottom of a Petri dish with Krazy Glue and the preparation was bathed in modified Van Harreveld's solution ("saline"; Van Harreveld, 1936), which consisted in mM: 195 NaCl, 5.4 KCl, 13.5 $CaCl_2$, 2.6 $MgCl_2$ and 10 4-[2-Hydroxyethyl]piperazine-1-ethanesulfonic acid (HEPES), titrated to pH 7.3 with NaOH. The ventral cuticle of the propodite segment was removed with forceps and spring scissors, followed by the closer muscle and any connective tissue found above the opener muscle. Great care was taken to avoid damaging the motor axons on the surface of the opener muscle while the connective tissue was removed (Figure 3). Lastly, the entire cuticle of the meropodite segment was removed from the meropodite/carpopodite joint to expose the nerve bundles innervating the opener muscle. Using forceps, the nerve bundle containing the excitatory opener nerve was separated from the bundle containing the inhibitory opener nerve. This allowed for later, selective stimulation of the excitatory axon.

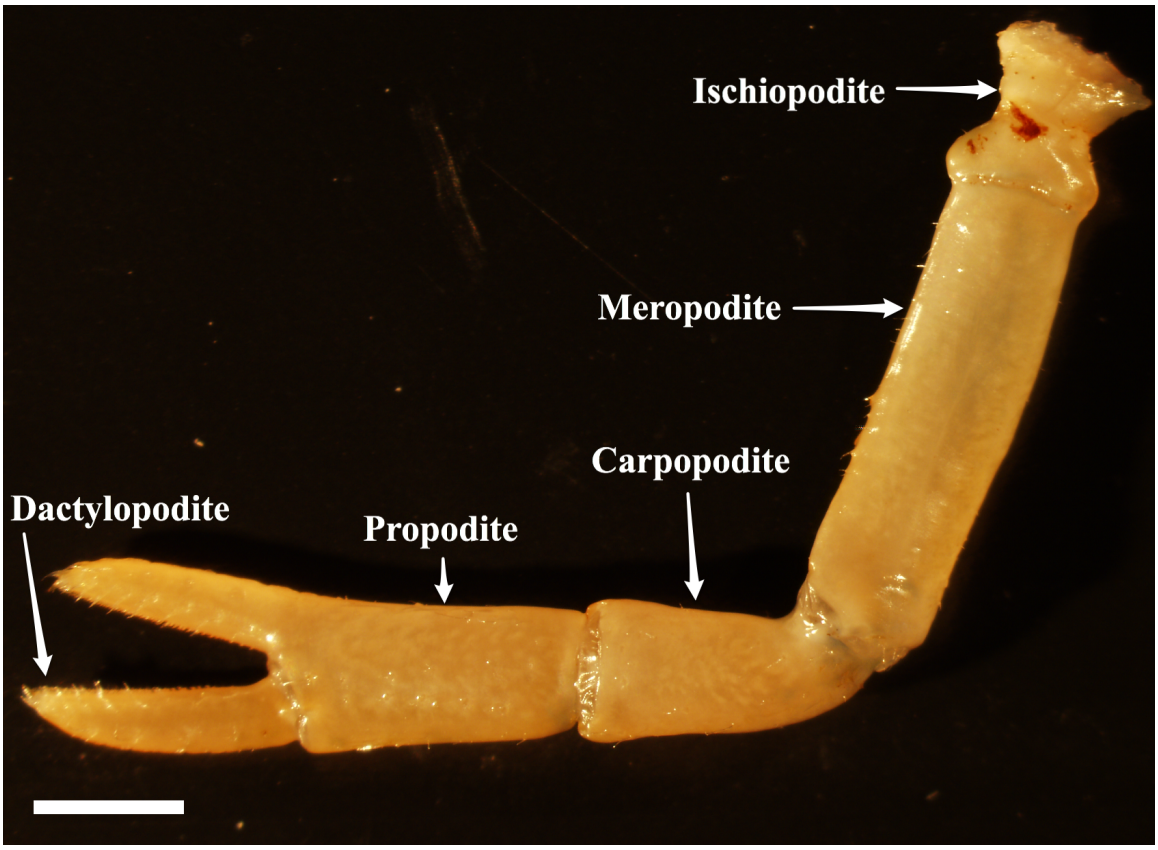

Figure 2. The first walking leg of the crayfish. The claw opener muscle is located in the propodite segment. The excitatory axon is stimulated in the meropodite segment. Stimulation of the opener muscle results in abduction of the dactylopodite. Scale bar = 2 mm.

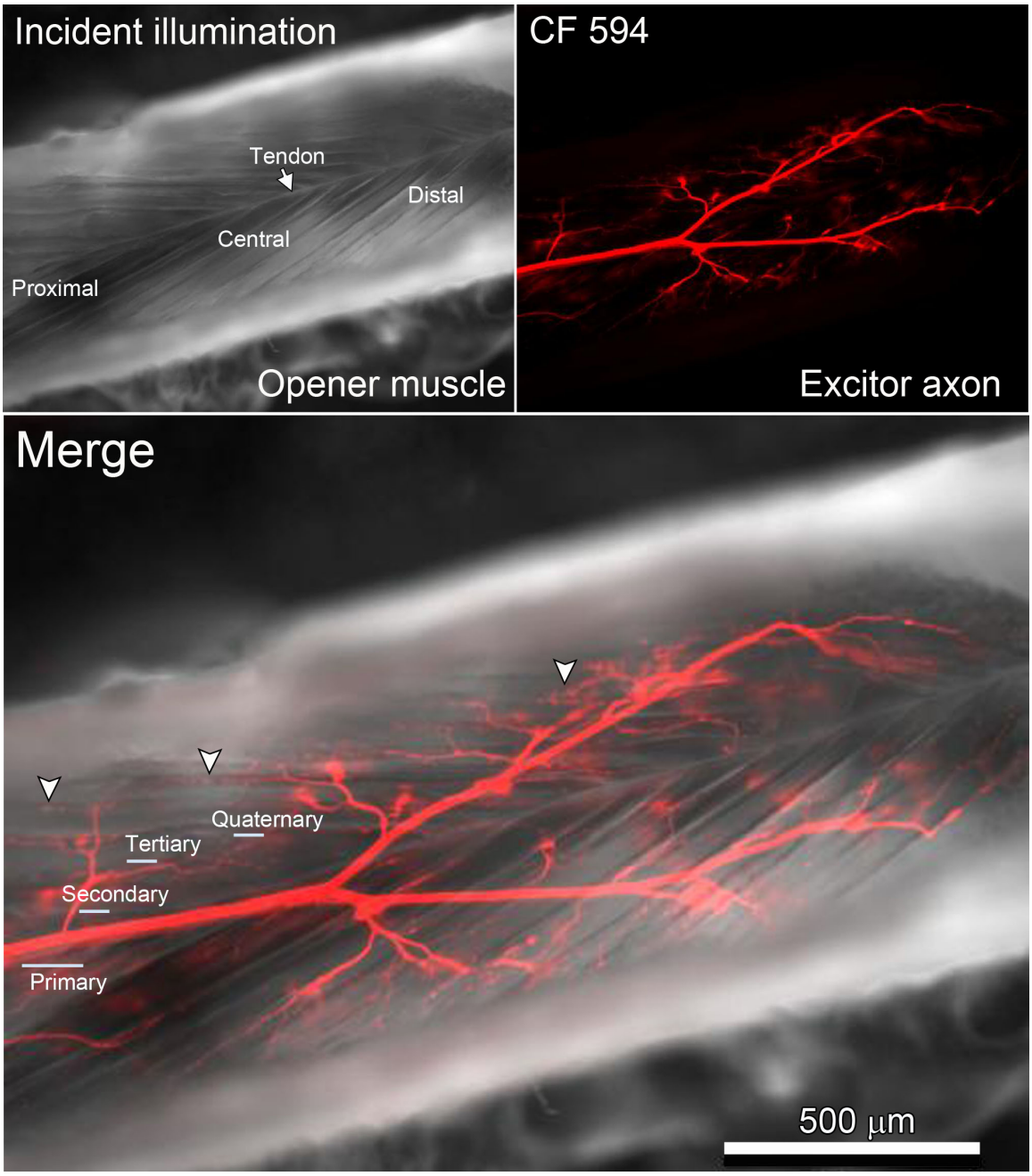

Figure 3. Claw opener neuromuscular junction. The dactyl (claw) opener muscle fibers are innervated by an excitatory axon (top right) and an inhibitory axon (not labeled). The axons branch to make synaptic contacts with multiple regions of every fiber of the muscle (arrow heads).

2.2 Experimental Setup and Electrophysiology

Preparations were placed on a X-Y translation stage under an upright Olympus BX51WI epifluorescence microscope. The preparations were kept at room temperature. The excitatory ('excitor') nerve from the meropodite segment was stimulated via a glass suction electrode. This consisted of a fire-polished glass capillary tube large enough for the nerve bundle to enter, connected to a syringe by fine tubing to allow suction to be applied. The excitatory nerve bundles were sucked into the tube with crayfish saline and the stimulus was applied between the inside and outside of the glass tube. Supra-threshold current pulses (one millisecond duration) were delivered from a PG4000 Digital Stimulator (Neuro Data Instruments Corp.) through a stimulus isolation unit (SIU 90, Neuro Data Instruments Corp.). Postsynaptic excitatory junction potentials (EJPs) were monitored on a Tektronix oscilloscope in every experiment to ensure that transmitter release was occurring. EJPs were measured with sharp (10-20 MΩ resistance) intracellular electrodes filled with 3 M KCl. EJPs were recorded with a custom-built high-impedance head stage amplifier, amplified a total of 100-fold, filtered between 0.3-300 Hz and digitally sampled at 4 kHz. Waves were acquired using SuperScope II software (v2.17.1, GW Instruments, Inc.) and analyzed offline using IgorPro (v6.31, Wavemetrics, Inc., Lake Oswego, OR).

Chapter 3 – Neuromodulation of Synaptic Vesicle Recycling Examined with FM1-43 Fluorescence Imaging

3.1 Introduction

Serotonin increases the release of neurotransmitter-containing synaptic vesicles from crayfish axon terminals, as described in 1.2. To allow for sustained enhancement of glutamate release at the crayfish opener NMJ, serotonin increases the number of vesicles available for release as determined by FM1-43 dye imaging (Wang and Zucker, 1998). FM1-43 is a fluorescent dye that has been widely used to image synaptic vesicle endocytosis and exocytosis (Gaffield and Betz, 2006). Wang and Zucker (1998) induced endocytosis by nerve stimulation and compared the fluorescence intensity of FM1-43 in presynaptic axon terminals. They found that the initial intensity of FM1-43-loaded terminals was significantly higher in serotonin conditions compared with controls. They then applied a second stimulus to cause exocytosis of vesicles and measured unloading of FM1-43 dye (during exocytosis) as a decay in fluorescence intensity. Interestingly, the rate of fluorescence decay was not significantly different between serotonin and control conditions, suggesting that the recycling kinetics were not changed by serotonin. Using their FM1-43 unloading data combined with EJP recordings, the authors calculated the number of vesicles available for synaptic transmission and found that the increased fluorescence intensity in the presence of serotonin was caused by an increase in the recycling pool size.

Wang and Zucker (1998) further demonstrated that if serotonin were removed from the system after FM1-43 loading, a percentage of the labeled vesicles would fail to exocytose during the unloading stimulus. The authors stimulated endocytosis in the presence of serotonin and, after waiting for the effects of serotonin to wear off, stimulated exocytosis. They measured exocytosis as a decrease in FM1-43 fluorescence during the unloading stimulation and found that a higher percentage of fluorescence *remained inside the axon terminals* at the end of the stimulus compared to their control. The authors

results suggest that serotonin is able to activate a population of previously non-recycling vesicles. Furthermore, when the effects of serotonin have decayed away, a proportion of the activated vesicles appear to return to a non-releasable state.

Thus, it was hypothesized that serotonin activates a non-recycling population of synaptic vesicles within the presynaptic vesicle cluster. Specifically, it was predicted that serotonin will recruit functionally non-releasable (reserve) vesicles to become releasable (recycling). This assumption is intuitive because estimates of vesicle pool sizes at frog and *Drosophila* NMJs, as well as cultured hippocampal neurons, indicated that the reserve pool is significantly larger than the recycling pool (Delgado et al., 2000; Harata et al., 2001; Richards et al., 2000; Rizzoli and Betz, 2004*)*, therefore vesicles could easily be recruited within the vesicle cluster. If recruitment occurs then once serotonin is removed from the system some previously activated vesicles could return to a reserve state. This hypothesis is supported by Wang and Zucker's results showing that a fraction of FM1-43 taken up during stimulation failed to unload upon removal of serotonin. Our first aim, therefore, was to confirm Wang and Zucker's results using their FM1-43 dye unloading technique. Our second aim was to locate the serotonin-activated (and deactivated) synaptic vesicles within axon terminals using photoconversion of FM1-43 and transmission electron microscopy techniques.

3.2 Materials and Methods

The preparation of animals, experimental setup and electrophysiology were performed as reported in Chapter 2 – General Materials and Methods.

3.2.1 Exogenous application of serotonin and EJP recordings

Stock serotonin (1 mM in crayfish saline; H9523, Sigma-Aldrich Co.) was pipetted directly into the preparation bath for a final concentration of 5 μM. Serotonin was bath applied for 10 minutes prior to the onset of labeling synaptic vesicles with FM1-43 dye.

To ensure that serotonin increased transmitter release during axonal stimulation, EJPs were monitored on an oscilloscope.

3.2.2 FM1-43 loading and unloading

FM1-43 is a water-soluble non-toxic dye with a structure ideally suited for labeling recycling synaptic vesicles (Figure 4A; Betz et al., 1992). When applied extracellularly, the lipophilic tail region of the dye inserts into the lipid portion of the axon membrane and is taken up during endocytosis of vesicles and endosomes (Figure 4B). The FM1-43 molecule has a charged head region that prevents complete passage of the dye through the membrane. As a result, FM1-43 dye captured through endocytosis remains trapped inside the lumen of the vesicles until exocytosis. The fluorescence properties of the dye lie in the core region; the fluorescence increases significantly upon insertion of the molecule into the lipid bilayer (Wu et al., 2009). Once extracellular dye has been rinsed away, FM1-43-labeled vesicles can be imaged with fluorescence microscopy. Additionally, release of FM1-43-dye via vesicle exocytosis can be recorded as a decrease in fluorescence intensity over time. The decay of fluorescence corresponds to the departitioning of the dye from the membrane (Neves and Lagnado, 1999; Richards et al., 2005). FM1-43 is preferentially used because of its high signal to noise ratio (Wu et al., 2009).

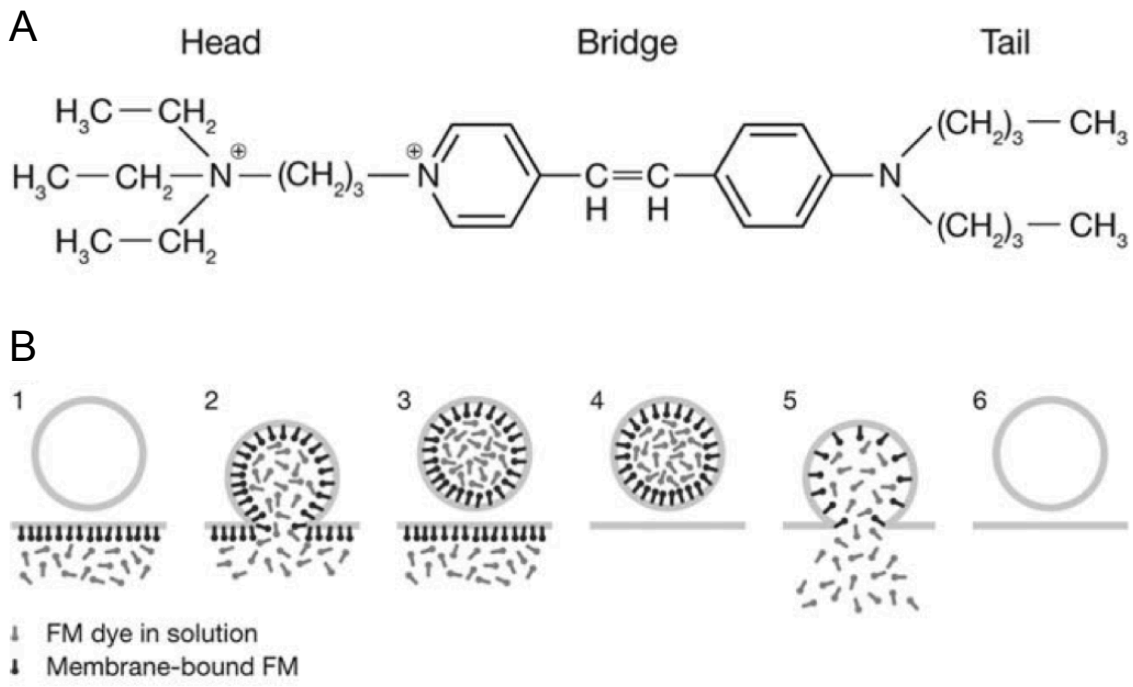

Figure 4. FM1-43 has a structure ideally suited for labeling recycling vesicles. (A) The FM1-43 molecule is composed of a lipophilic tail that partitions into cell membranes and a positively charged head region, which prevents complete permeation of membranes. The middle region contains two aromatic rings that create the fluorophore. The number of double bonds in the bridge connecting the two rings determines the spectral characteristics of the dye. **(B)** (1) Bath-applied FM1-43 molecules partition into cell membranes. (2 & 3) Stimulated endocytosis causes FM1-43 dye to be taken up inside newly formed vesicles and endosomes (loading). (4) The dye can be washed from the extracellular solution but remains inside loaded vesicles. (5) Preparations re-stimulated will exocytose FM1-43-loaded vesicles and the dye will be released into the extracellular solution (unloading). (6) Axon terminals can be reloaded with FM1-43 dye after complete unloading. Modified from Hoopmann et al., 2012.

FM1-43 loading and unloading protocol

Recycling synaptic vesicles were labeled with the fixable analog of the fluorescent styryl dye FM1-43 (FM1-43FX, Molecular Probes, Eugene, OR). The general loading and unloading protocol used for the FM1-43-labeling experiments is depicted in Figure 5.

Stock FM1-43 (1 mM in crayfish saline) was bath applied for a final concentration of 10-15 μM and allowed to equilibrate around the preparation for 5 minutes before loading. To load FM1-43, the excitor axon was stimulated continuously at 20 Hz for 3 minutes. Upon cessation of the 20 Hz loading stimulus, the sulfonated β-cyclodextrin derivative ADVASEP-7 (10 mM stock in crayfish saline) was bath applied for a final concentration of 1 mM for 1 minute to scavenge the non-endocytosed FM1-43. ADVASEP-7 has a higher affinity for FM1-43 than the plasma membrane and helped to reduce the background fluorescence caused by FM1-43 bound to the outer leaflet of the plasma membranes (Gaffield and Betz, 2006; Kay et al., 1999). The preparation was then rinsed with dye-free saline via gravity perfusion system to wash excess dye. The rate of perfusion was controlled at 1 mL/min. The time spent rinsing was varied, depending on the experiment performed (typically 30-180 minutes). After rinsing, the preparations were unloaded with a continuous 20 Hz tetanus for up to 1 hour.

For some experiments, the loading and unloading of FM1-43 occurred in the presence of serotonin. In those experiments, serotonin was bath applied for 10 minutes prior to, and during, the loading stimulus (Wang and Zucker, 1998). The preparations were then rinsed in dye- and serotonin-free saline. Stimulated unloading of labeled terminals occurred either in the presence or absence of serotonin, depending on the experimental condition (Figure 5).

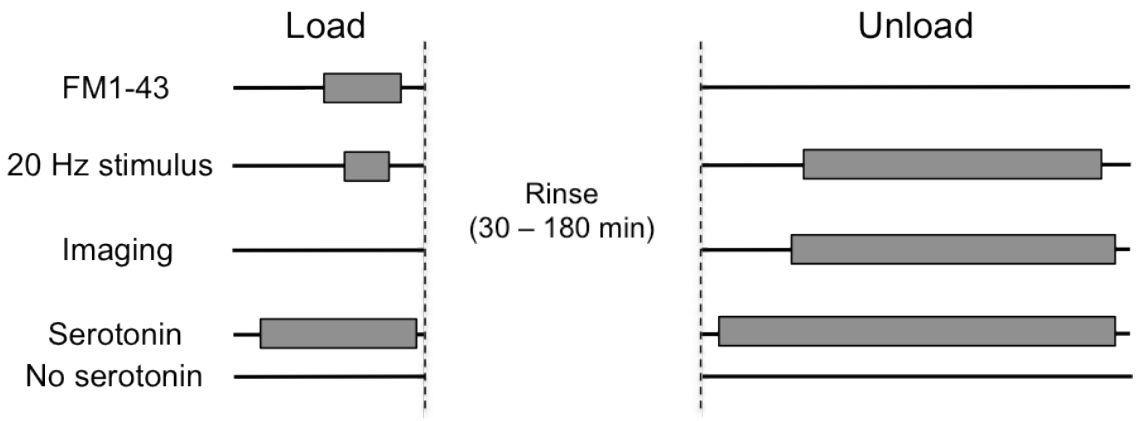

Figure 5. FM1-43 loading and unloading protocol. Vesicles undergoing endocytosis were labeled by bath application of 10-15 μM FM1-43 and 20-Hz axonal stimulation (loading). Preparations were then rinsed for varied lengths of time to remove non-vesicular membrane-bound dye before the fluorescence signal was imaged. FM1-43-labeled vesicles were exocytosed with 20-Hz continuous axonal stimulation in dye-free saline (unloading). The decrease in fluorescence intensity corresponding with vesicle fusion was measured with frequent image capture. When serotonin was included, 5 μM was bath-applied for 10 minutes prior to both loading and unloading.

3.2.3 Optical measurements and microscopy

FM1-43-labeled terminals on the opener muscle were viewed with an Olympus LUMPlanFl/IR 40X/0.80 NA water objective. The preparations were illuminated using a 75W Xe-lamp coupled to a Polychrome II switching monochrometer (T.I.L.L. Photonics GmbH). FM1-43 was excited at 475 nm and emission was detected with a 500-600 nm filter. Images were captured with an Evolve 512 EMCCD camera (Photometrics, Tuscon, AZ) connected to Micro-Manager software (Edelstein et al., 2010) on a PC.

Images were acquired immediately prior to, and frequently during, the 20-Hz unloading tetanus. Several terminals were typically imaged at a time, within ~100 μm diameter field of view, restricted by a field stop aperture. Analysis was performed in

ImageJ (Abràmoff et al., 2004). Images collected prior to, and during, the unloading tetanus were organized by time in an image stack. The freehand selection tool was used to outline discrete, focused, FM1-43 puncta and the mean intensity of the regions of interest (ROI) was calculated for all images in the stack. In each experiment the mean intensities from 5-15 puncta were averaged for each time point. Background measurements were also obtained at each time point from nearby axon branches void of FM1-43 puncta. Mean background fluorescence values were subtracted from averaged mean FM1-43 intensities and the data was normalized to the first time point (i.e. loaded terminals or time = 0 min) to allow for grouping of multiple experiments. The equation used was $((F_{t0\text{-}t50} - B) / (F_{t0} - B))$.

The decay of FM1-43 fluorescence during 20-Hz continuous stimulation was plotted from the normalized averages of at least 5 animals. Due to muscle contraction during the 20-Hz unloading stimulation, focused images could not be obtained at set times in all experiments. As a consequence, averaging multiple experiments was difficult. In order to obtain an average of all experiments, a cubic spline interpolation was applied using Igor Pro's wave analysis software (WaveMetrics, Lake Oswego, OR, USA) and fluorescence intensity values were determined for set time points (one value per minute). The means and variation of the means were calculated from the interpolated spline functions.

The rate of FM1-43 fluorescence unloading (τ) was determined from 1st order exponential functions fit to each experiment. Mean τ values were calculated for each group. The means of the spline interpolations were also fit with 1st order exponentials to determine τ.

3.2.4 Statistical analysis

Statistical analysis was conducted using Prism 5 software (Graphpad Software Inc., La Jolla, CA). Data are presented as means ±standard error of the mean (SEM). Percent

of remaining fluorescence intensity after 20-Hz stimulation and rates of unloading were assessed using one-way ANOVAs and multiple comparisons were made using the Tukey-Kramer post-test. P-values of <0.05 were considered significant for all statistical tests.

3.3 Results

3.3.1 Serotonin increases the release of the neurotransmitter glutamate

To demonstrate the enhancement of glutamate release by serotonin, EJPs were recorded with sharp intracellular electrodes. Three legs were stimulated with 20 Hz trains of 10 axonal stimulations and EJPs were recorded before (control) and after application of serotonin (Figure 6A). Normalized and pooled data revealed that the amplitudes of all EJPs were significantly larger after serotonin was applied (paired t-test, $P < 0.01$, $N = 3$ legs). The amount of facilitation of the EJPs during the stimulus trains was not changed by application of serotonin (Figure 6B).

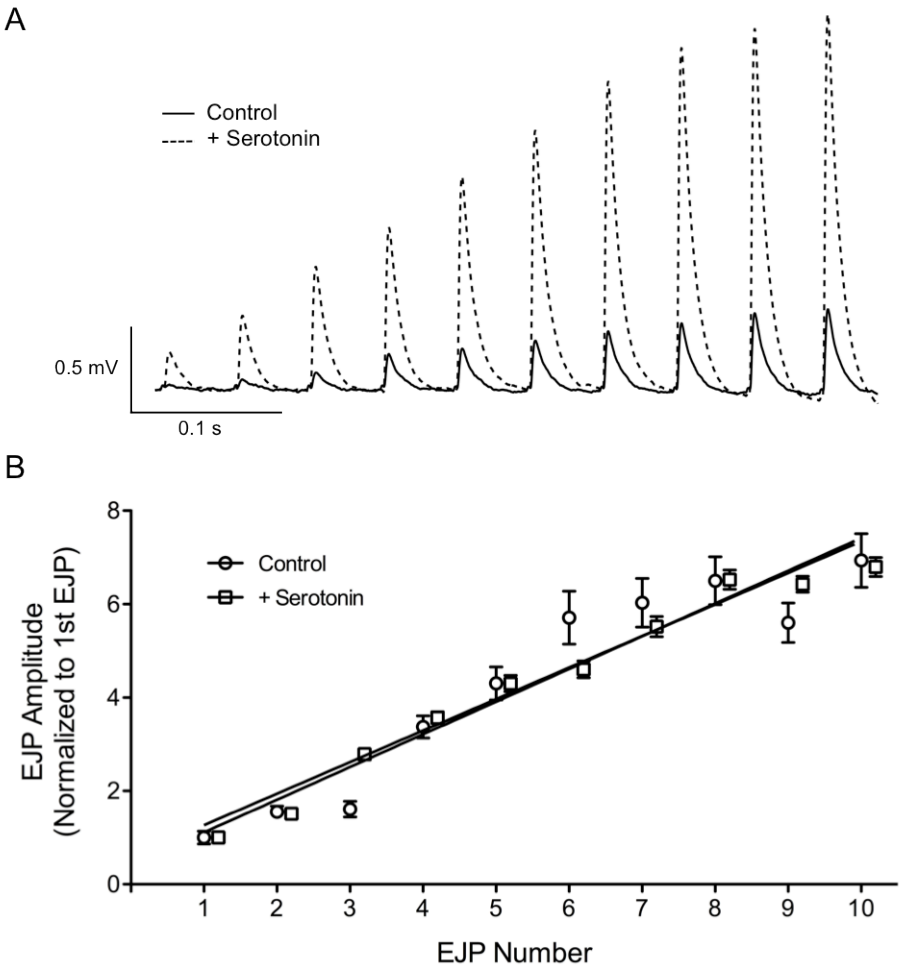

Figure 6. Brief application of serotonin produces large increases in EJP amplitudes but does not alter facilitation of EJPs. The excitor axon was stimulated with a 20 Hz train of 10 axonal stimulations. (A) EJPs before (control) and after 10 minute incubation with 5 μM serotonin show marked increases in amplitudes. Each trace is an average of 40 stimulus trains. (B) The amount of facilitation of EJPs is not changed during exposure to serotonin. Means ±SEM for 40 stimulus trains of EJPs recorded before (open circles) and after serotonin (open squares). Fitted lines are linear regressions: r^2=0.9 for control and r^2=0.97 for serotonin.

3.3.2 Testing recruitment of vesicles by serotonin with FM1-43 unloading

FM1-43 unloading was used to test the hypothesis that serotonin increases the total number of recycling vesicles by recruiting non-recycling vesicles. To replicate Wang and Zucker's (1998) results, vesicles were loaded with FM1-43 in the presence of serotonin. After FM1-43 loading, the preparations were rinsed with dye-free crayfish saline for 90 minutes to allow for the effects of serotonin to wear off. The FM1-43-labeled vesicles were then unloaded in serotonin-free saline until the fluorescence plateaued. We predicted that a proportion of vesicles activated by serotonin would resume non-recycling (reserve) status once serotonin was removed from the system. This population of vesicles would be expressed as higher remaining fluorescence intensity at the end of the unloading stimulus compared to groups that did not have serotonin removed after the loading stimulus.

I compared the serotonin load/saline unload group (Ser/Sal) with one group that had FM1-43 loaded and unloaded in the presence of serotonin (Ser/Ser) and a second group that had FM1-43 loaded and unloaded in the absence of serotonin (Sal/Sal). We predicted that the Ser/Sal group would result in more remaining fluorescence at the end of the unloading stimulus compared to both Ser/Ser and Sal/Sal groups. Fluorescence images of FM1-43 loaded and at various stages of unloading are shown in Figure 7. The decay of FM1-43 fluorescence for the Ser/Sal, Ser/Ser and Sal/Sal groups are plotted in Figure 8A, B and C, respectively. The fluorescence decays of individual experiments are shown in each panel along with the means of the spline fits (thick lines). Figure 8D overlays the spline-fit means of the three groups for visual comparison.

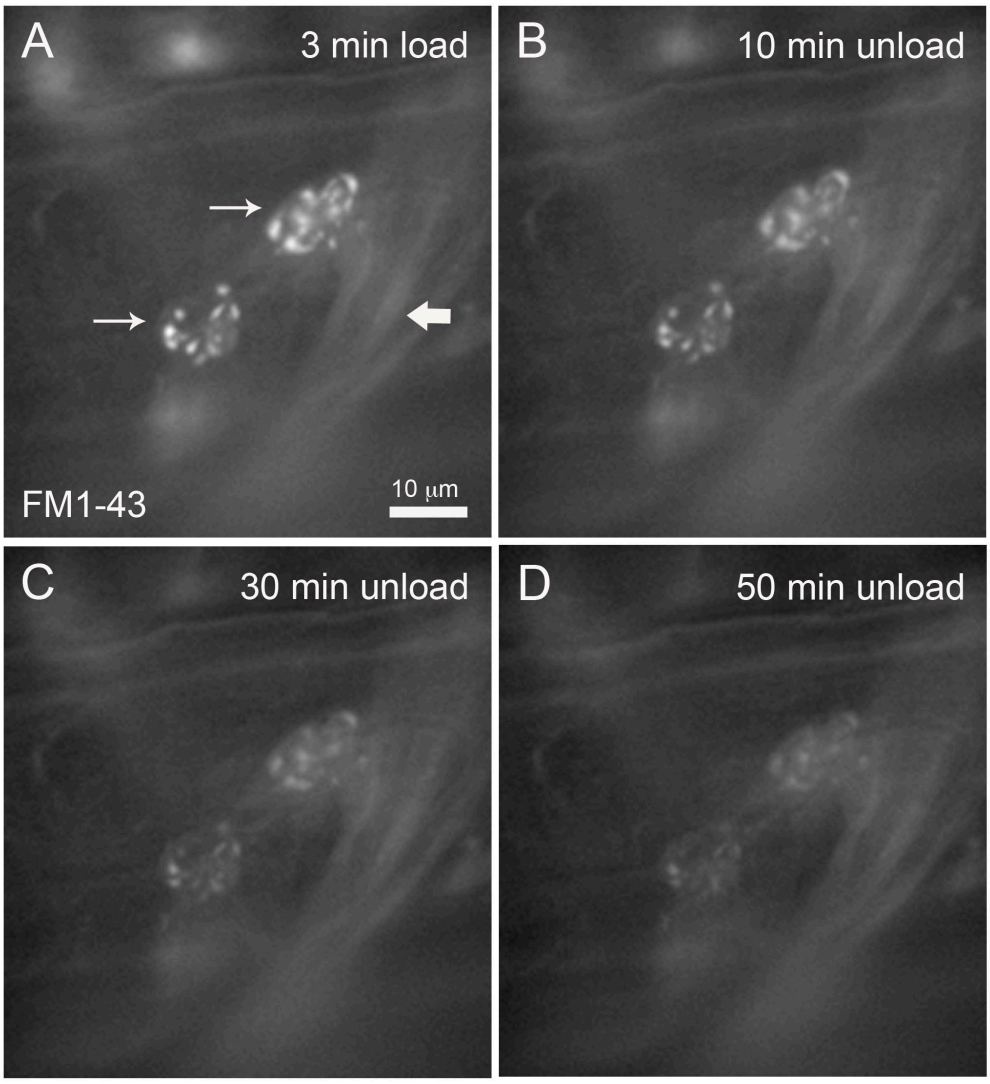

Figure 7. Fluorescence images of FM1-43 loading and unloading in crayfish axon terminals. (A) Recycling vesicles were loaded with FM1-43 in normal crayfish saline. The FM1-43 puncta in the field of view are located inside two axon terminals (small arrows) that are budding from an axon branch (large white arrow). Each FM1-43 punctum represents active zones containing recycling synaptic vesicles. Preparations were rinsed for 90 minutes and the axons were restimulated in dye-free saline to unload FM1-43. (B-D) The fluorescence of FM1-43 puncta decreased during the unloading stimulation as dye-labeled vesicles exocytosed. FM1-43 puncta are still visible by 50 minutes of unloading.

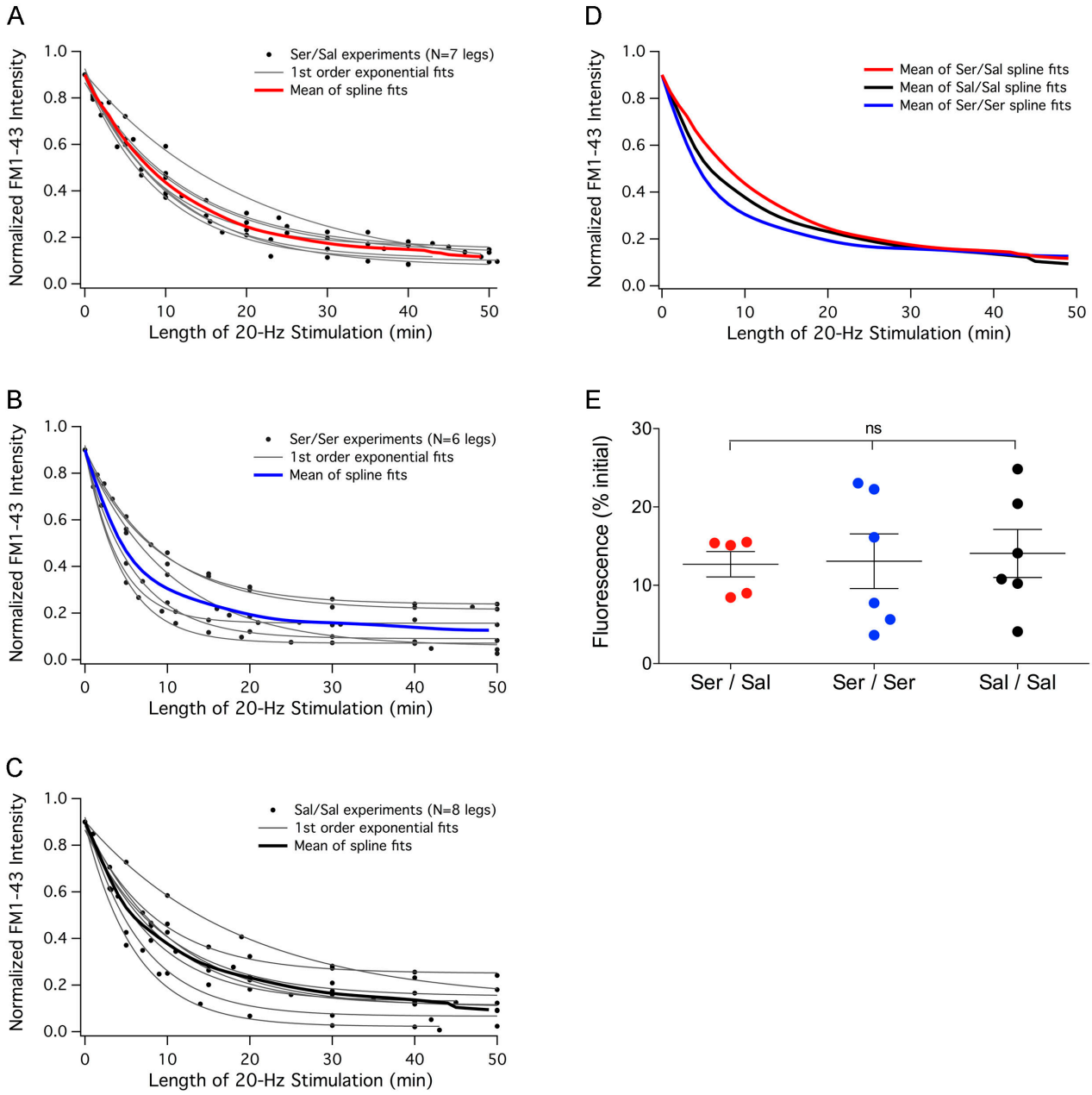

Figure 8. A distinct serotonin-activated population of vesicles could not be resolved with FM1-43 unloading. (A-C) Dye unloading in Ser/Sal, Ser/Ser and Sal/Sal groups, respectively. Individual experiments (filled circles and thin lines) are shown along with the means of the spline interpolations (thick lines). (D) The mean unloading curves show similar amounts of FM1-43 destaining by ~30 minutes of 20-Hz stimulation. (E) The percentage of remaining fluorescence, determined from the last 10 minutes of unloading, was not statistically different among the three groups (P = 0.94, one-way ANOVA).

The percentage of remaining fluorescence was calculated as the mean ±SEM of the individual spline interpolations during the last 10 minutes of stimulation (Figure 8E). We found that 12.7 ±1.6% of dye could not be unloaded from preparations that had serotonin included for loading but excluded during unloading (Ser/Sal: N = 5 legs) compared to preparations that included serotonin in both loading and unloading (Ser/Ser: 13.1 ±3.5%, N = 6 legs) and preparations that excluded serotonin from both loading and unloading (Sal/Sal: 14.1 ±3.1%, N = 6 legs). The amount of remaining fluorescence was not statistically different among the three groups (one-way ANOVA, P = 0.94).

The rate of dye unloading (τ) was assessed by fitting 1st order exponentials to the individual experiments and then calculating the mean ±SEM. The rate of unloading in the group that had serotonin present for loading but removed for unloading (Ser/Sal: τ = 12.0 ±1.5 min, N = 7) was not statistically different from the group containing serotonin in both loading and unloading (Ser/Ser: τ = 7.0 ±1.1 min, N = 6) or the group excluding serotonin from both loading and unloading (Sal/Sal: τ = 9.7 ±1.4 min, N = 8) (one-way ANOVA, P = 0.07). The rate of dye unloading was also assessed by fitting 1st order exponential functions to the means of the spline interpolations (Ser/Sal τ = 11.2 min; Ser/Ser τ = 6.6 min; Sal/Sal τ = 9.4 min). Both methods revealed a faster rate of FM1-43 unloading when serotonin was present during the unloading stimulus (Ser/Ser). This was likely a result of enhanced release kinetics and/or the release of more vesicles per action potential (Southard et al., 2000; Vyshedskiy et al., 1998).

To determine whether photobleaching affected FM1-43 unloading, four legs were loaded with FM1-43 (3 minutes, 20 Hz) and after 30 minutes of dye-free rinsing the labeled terminals were imaged every 6 seconds in the absence of stimulation. At least 20 images were captured to correspond with the number of images collected during the unloading experiments. Mean intensity of the FM1-43 puncta decreased by less than one percent (0.58 ±0.60%) over the course of the photobleaching experiments and thus, it was concluded that photobleaching had very little affect on the fluorescence measured during unloading.

This FM1-43 unloading experiment was unable to reveal a distinct serotonin-activated population of synaptic vesicles. Synapses loaded with FM1-43 in the presence of serotonin did not retain a statistically higher percentage of dye after unloading in serotonin-free saline compared to groups that had either serotonin present during loading and unloading, or serotonin absent during loading and unloading. This is in contrast to a previous report that suggested axon terminals retain a statistically higher percentage of FM1-43 when serotonin is present for loading but removed during unloading, compared to preparations that had serotonin absent for both loading and unloading (Wang and Zucker, 1998).

3.3.3 The delay between FM1-43 loading and unloading affects both the amount and the kinetics of unloading

Our FM1-43 unloading experiment had two differences from Wang and Zucker's (1998) experiment that we thought might be able to explain the discrepancy in results. First, the length of our unloading stimulation was approximately double the length of the stimulation in the previous study (50 min vs. 26 min), which we believe accounts for the difference in amount of unloading reported (~23% vs. ~13%). Importantly, we determined the percentage of FM1-43 fluorescence remaining at ~26 minutes of unloading in our study to be ~20%, in agreement with their report of ~23% at that time. Our study shows that more FM1-43 can be released from vesicles when a longer unloading stimulation is provided. Second, whereas our study compared three groups (Ser/Sal, Ser/Ser, and Sal/Sal) that all had 90 minutes of delay between dye loading and unloading, Wang and Zucker compared their Ser/Sal group (90 minute delay) to a Sal/Sal group with only a 40-minute delay between loading and unloading. It was hypothesized that it was the *time* between loading and unloading that affected the ability for labeled vesicles to be re-released, not serotonin. It was predicted that endocytic vesicles would initially be located close to release sites, but over time the vesicles would diffuse to farther regions of the synapse or intermix with the main reserve cluster. Therefore, the proximity of FM1-43-labeled vesicles to release sites at early time points would result in

unloading of more FM1-43 fluorescence at a relatively faster rate compared to FM1-43-labeled vesicles that had diffused around the synapse and associated with the main vesicle cluster over time. It was also postulated that some of the dye-labeled vesicles might mature into the main cluster and thus be less likely to exocytose during an unloading stimulus. Vesicles that failed to exocytose, and therefore unload the FM1-43 dye, would result in higher remaining fluorescence intensity inside the terminals at the end of unloading.

To test the hypothesis of vesicle redistribution, the length of time was changed between loading and unloading FM1-43. Groups that had 30- and 180 minutes of rinsing between loading and unloading were compared. The lengths of the loading and unloading stimulations, and the frequency of stimulations were the same as the previous experiment, but serotonin was not included. The percentage of dye remaining inside the terminals at the end of 20-Hz unloading and the rate of fluorescence decay during the unloading stimulus was measured. Representative fluorescence images of FM1-43 loaded and at different stages of unloading are shown in Figure 9.

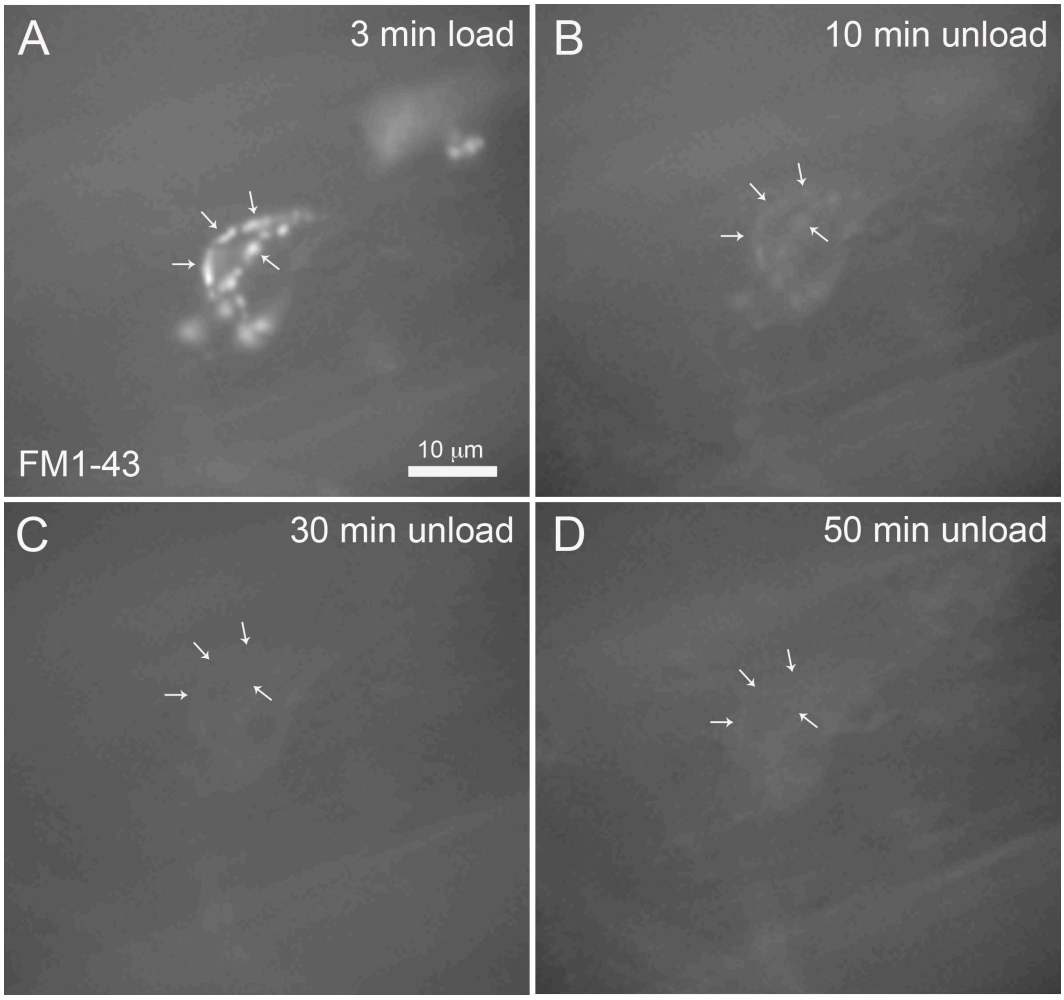

Figure 9. Fluorescence images of FM1-43 loading and unloading after a 30-minute delay. (A) Recycling vesicles were loaded with FM1-43 in normal crayfish saline. The FM1-43 puncta (arrows) in the field of view are located inside one axon terminal. Each FM1-43 punctum represents an active zone with recycling synaptic vesicles. Preparations were rinsed for 30 minutes and the axons were restimulated in dye-free saline to unload FM1-43. (B-D) The fluorescence of FM1-43 puncta decreased during the unloading stimulation as labeled vesicles exocytosed. No visible fluorescence from the FM1-43 puncta remained after 30 minutes of unloading.

The fluorescence lost during the delay between loading and unloading was also determined, because the delay varied between the groups (Figure 10A). Three preparations were loaded (3 minutes, 20 Hz) with FM1-43 and mean fluorescence intensity was measured during 180 minutes of resting (no stimulation) and normalized to

time = 30 minutes after the loading stimulus. It was found that after 180 minutes of delay, 69.1 ±4.2% of fluorescence remained. Thus over the course of 180 minutes, approximately 30% of FM1-43 dye was lost. The linear rate of fluorescence decay observed is expected with spontaneous vesicle release at a frequency of ~ 1/second.

Unloading of FM1-43 in the 30- and 180-minute delay conditions is shown in Figure 10B and 10C, respectively. Individual experiments are shown (filled circles and thin lines) along with the means of the spline interpolations from the experiments (thick lines). Figure 10D overlays the means of the spline interpolations for the 30- and 180-minute delay groups, normalized to 30- and 180-minutes following the loading stimulus, respectively. Figure 10E overlays the means of the spline interpolations for the two groups, both normalized to 30 minutes following the loading stimulus.

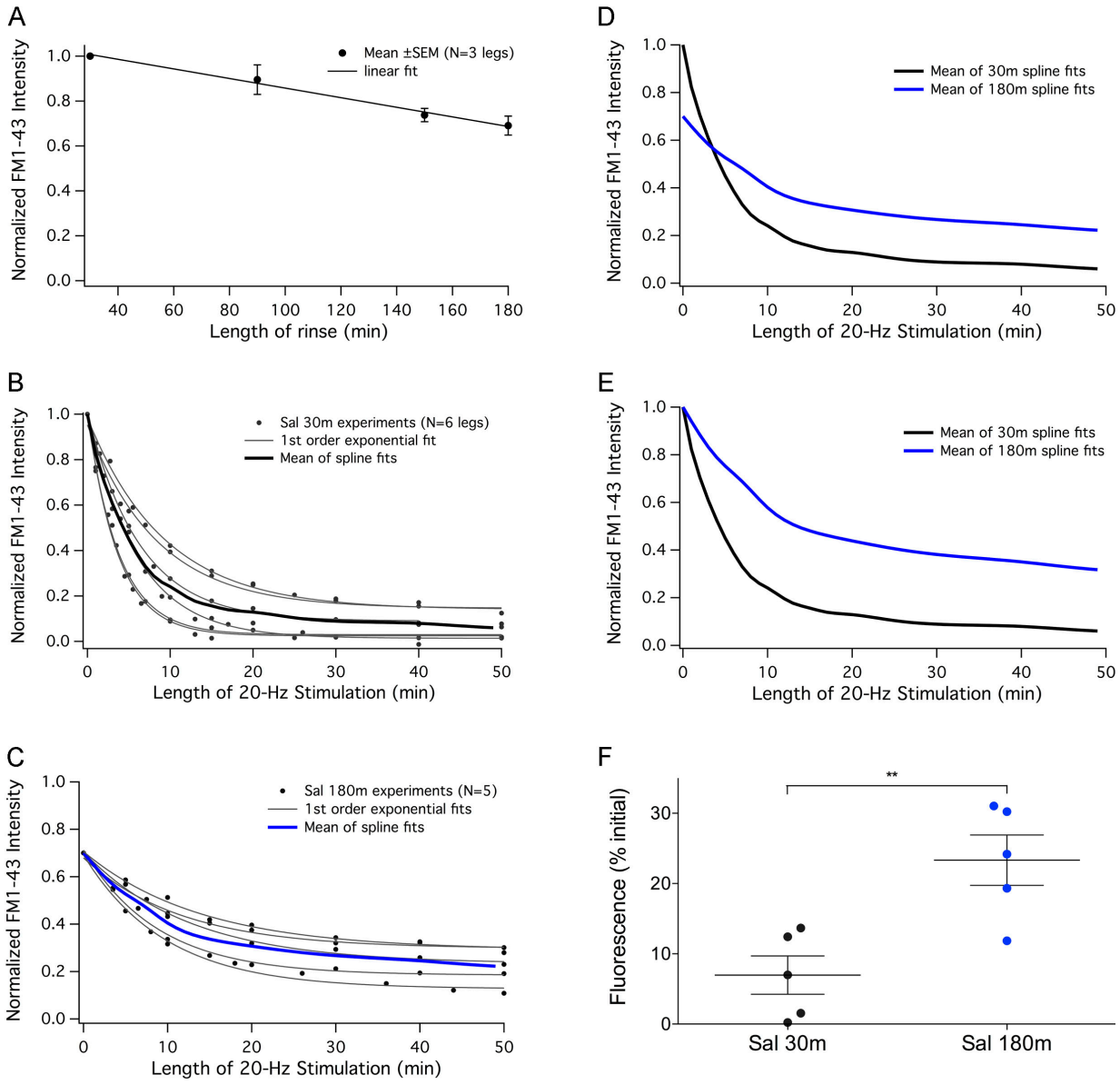

Figure 10. The delay between loading and unloading FM1-43 affects the amount of dye unloaded. (A) Fluorescence decay during 180 minutes of rinsing (no stimulation), normalized to 30 minutes following the end of the loading stimulus. r^2= 0.99 for linear fit. (B-E) FM1-43 unloading after 30- and 180-minute delays, respectively. The initial fluorescence (B, C, D) is adjusted to represent the percentage of dye lost during the delay in (A). (E) Initial fluorescence is normalized to 30 minutes following the end of the loading stimulus. (F) The percentage of remaining fluorescence, calculated from the last ten minutes of 20-Hz unloading, is statistically higher after a 180-minute delay compared to a 30-minute delay (** P <0.01, one-way ANOVA and Tukey-Kramer post-test).

The percentage of remaining fluorescence was calculated as the mean ±SEM of the individual spline interpolations during the last 10 minutes of stimulation (Figure 10F). It was found that 7.0 ±2.7% of dye remained with a 30-minute delay (N = 5 legs) compared to 23.3 ±3.6% (N = 5 legs) with a 180 minute delay. As the length of the delay increased, more FM1-43 fluorescence remained inside the terminals at the end of the unloading stimulus. There was statistically more fluorescence remaining in the 180-minute delay compared with the 30-minute delay ($P < 0.01$, one-way ANOVA and Tukey-Kramer post-test).

The rate of dye unloading (τ) was assessed by fitting 1st order exponentials to the individual experiments and determining the mean ±SEM of the exponentials for each group. The rate of unloading in the 30-minute delay group (τ = 6.2 ±0.9 min, N=6 legs) was statistically faster than the 180-minute delay group (τ = 11.3 ±0.9 min, N=5 legs)($P < 0.05$, one-way ANOVA and Tukey-Kramer post-test). The rate of dye unloading was also assessed by fitting 1st order exponential functions to the means of the spline interpolations (30-min τ = 5.7 min; 180-min τ = 10.5 min). Both methods revealed that the rate of dye unloading slowed as the duration of the delay was increased.

This experiment illustrated that a significant percentage of vesicles labeled with FM1-43 lose their ability to be released, or take longer to release, if the unloading stimulus occurred hours later. The results showed that as the delay between loading and unloading was increased, the rate of dye unloading decreased and less dye could be unloaded.

3.4 Discussion

3.4.1 FM1-43 dye unloading does not reveal a serotonin-activated population of vesicles

A serotonin-activated population of synaptic vesicles could not be resolved with the FM1-43 fluorescence unloading technique. The percentage of remaining fluorescence at the end of the unloading stimulations was not significantly different among the Ser/Sal, Ser/Ser and Sal/Sal groups. It was determined, however, that the length of time between the loading and unloading stimulations changed the rate of FM1-43 unloading and the total percentage of dye able to be unloaded. When the delay was increased from 30 to 180 minutes, less FM1-43 dye was unloaded and at a slower rate.

Controlling the time of loading, washing and unloading is a crucial parameter in these fluorescence experiments. Wang and Zucker's (1998) study compared the Ser/Sal group with a 90-minute delay between dye loading/unloading to a Sal/Sal group with a 40-minute delay. They reported ~23% of dye could not be unloaded 90 minutes after washing out serotonin, compared to ~4.2% in their control with a 40 minute delay. We hypothesized that the difference in the percentage of remaining FM1-43 fluorescence was due to the length of the delay and not to the effects of serotonin.

The percentage of FM1-43 dye remaining in axon terminals at the end of our Ser/Sal experiment was lower than those obtained by Wang and Zucker (~13% vs. ~23%); however, our unloading stimulation was twice the length of theirs (50 min vs. 26 min). Importantly, the percentage of remaining fluorescence at 26 minutes of unloading in our experiment was ~20%, in agreement with their report. The 30-minute serotonin-free group in our experiment was also compared to the Wang and Zucker's 40-minute serotonin-free group, and both the percentage of remaining fluorescence and the rate of unloading were not statistically different. Therefore, this experiment reliably replicated some of the findings of Wang and Zucker (1998) and so differences are not due to methodology. Instead, it was apparent that the FM1-43 dye unloading technique used in

both studies was not suitable for testing if serotonin increased the number of recycling vesicles by recruiting non-recycling vesicles.

Neither this experiment nor the previous report (Wang and Zucker, 1998) identified a serotonin-activated population of synaptic vesicles. Instead of serotonin increasing the number of recycling vesicles, it appeared that the length of time between dye loading and unloading affected the behaviour of dye unloading.

3.4.2 Synaptic vesicles appear to move around terminals over time

In our experiments, as the time between FM1-43 loading and unloading was increased from 30-180 minutes, less dye was unloaded from axon terminals and the rate of dye unloading was slower. The loaded FM1-43 dye should be contained inside synaptic vesicles and so it can be assumed that the remaining fluorescence corresponded to vesicles unable to exocytose. This suggested that a fraction of the recycling vesicles labeled with FM1-43 become less releasable over time. The current results supported the hypothesis that recycling vesicles mature into reserve vesicles over time and we predicted that the unloadable vesicles potentially cross-linked into the main reserve cluster via tethering with vesicle-associated proteins like synapsin (Cesca et al., 2010; Siksou et al., 2007). If this was the case, then the fraction of FM1-43-loaded vesicles that have integrated the tightest would be unlikely to regain their mobility and be exocytosed during an unloading stimulus.

The vesicle maturation hypothesis is testable at the ultrastructural level. Newly formed vesicles would be mobile and able to diffuse freely, but should initially be found near or adjacent to release sites. The large reserve cluster might also function as a barrier (Denker et al., 2011b) to restrict the diffusion of recycling vesicles so that higher fractions are retained between the cluster and the release sites. A few FM1-43-loaded vesicles could associate with the outer edges of the reserve cluster at early time points after endocytosis. Over time, however, more FM1-43-loaded vesicles would integrate

further into the main vesicle cluster and as a result, relatively fewer labeled vesicles would be found near the release sites. This maturation hypothesis was tested in the following chapter by employing photoconversion of FM1-43 dye and transmission electron microscopy.

Chapter 4 – Synaptic Vesicle Distribution Investigated with FM1-43 Photoconversion and Transmission Electron Microscopy

4.1 Introduction

To test the hypothesis that recycling vesicles mature into reserve vesicles over time, the spatial distribution of FM1-43-labeled vesicles within the synapse cluster was examined at the ultrastructural level. Previous studies suggest that recently endocytosed vesicles are mobile, in contrast to immobile reserve vesicles (Kamin et al., 2010) that are tethered with vesicle-associated proteins (Cesca et al., 2010). Unfortunately, the protein tethers that bind synaptic vesicles are not well preserved with standard electron microscopy and fixation techniques (Siksou et al., 2007), and so the functional vesicle pools could not be differentiated based on tethering versus mobility in this study. Instead, we predicted that recently endocytosed vesicles would be located closer to release sites after endocytosis, but that over time the vesicles would mature and integrate into the main reserve cluster away from the release sites. The difference in vesicle distributions would likely be subtle, but retention of FM1-43-labeled vesicles near release sites at early times following stimulation would indicate spatial differentiation of functional vesicle pools at this synapse. A schematic predicting the location and functional identity of synaptic vesicles at early and late time points in a previously stimulated synapse is presented in Figure 11.

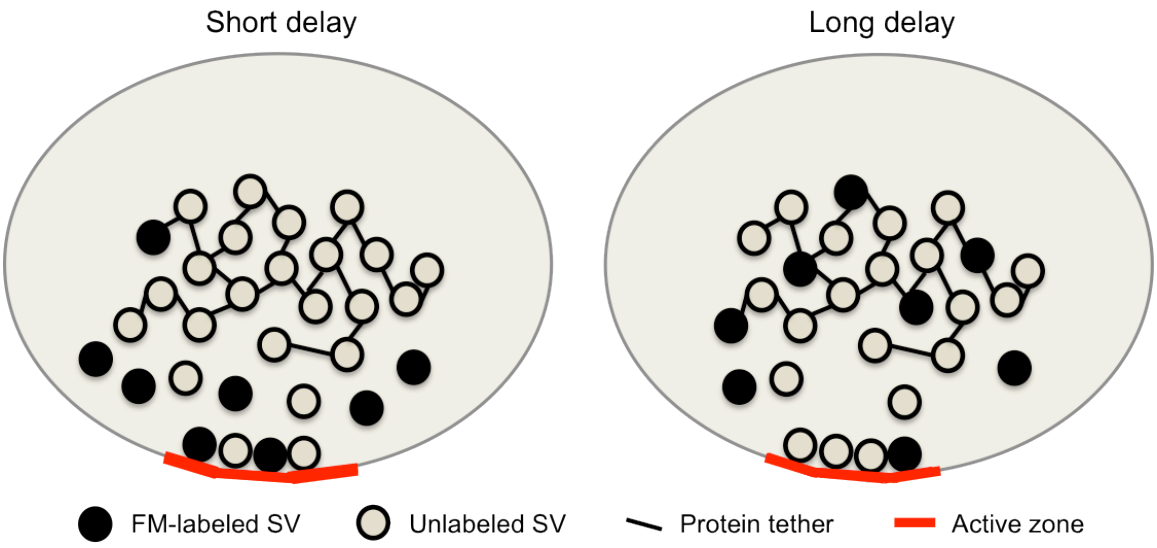

Figure 11. Schematic depicting predicted spatial distribution of FM1-43-labeled vesicles in crayfish terminals. Dye-labeled vesicles are located near release sites after endocytosis (left) but integrate into the main vesicle cluster over time (right).

This hypothesis suggests that a spatial distinction between recycling and reserve vesicles occurs at early time points. Association of endocytic (recycling) vesicles with sites of vesicle release have been observed at some synapses, e.g. at snake NMJs, endocytic vesicles were clustered near active zones, as determined through horseradish peroxidase labeling and photoconversion of FM1-43 (Teng and Wilkinson, 2000). In addition, synaptic vesicles labeled with ferritin tracer in goldfish bipolar neurons were found to be associated with synaptic ribbons (Paillart et al., 2003). At bipolar terminals, synaptic ribbons supply the releasable vesicles to the release sites. Spatial differentiation of recycling and reserve vesicles has not been observed in all synapses, however. At the frog NMJ, FM1-43 photoconverted recycling vesicles were scattered throughout the entire nerve terminal after brief stimulation (Rizzoli and Betz, 2004). In this experiment however, fixation occurred after a 10-minute delay following stimulation and thus allowed for vesicles to move to new locations. Therefore, the investigators also fixed their preparations immediately following stimulation and found an increase in the fraction of labeled vesicles located near the plasma membrane but not near release sites. In addition, previous reports at the *Drosophila* NMJ found that recycling and reserve vesicles were spatially separated using fluorescence imaging (Kuromi et al., 2004).

However, when the synapse was re-examined using electron microscopy photoconversion, the reserve and recycling vesicles were thoroughly intermixed (Denker et al., 2009). It is therefore possible that vesicle location is not relevant for functionality in all synapse preparations. Very little is known about functional vesicle pools in crayfish axon terminals and the results of the current experiment would contribute to the findings of the other synapse models.

To determine if there is evidence for spatially separated functional pools in crayfish axon terminals, photoconversion of FM1-43 to an electron dense precipitate and transmission electron microscopy techniques were employed. To determine spatial separation of vesicles, terminals containing FM1-43-labeled recycling vesicles were fixed at early time points after dye loading and terminals were examined for retention of labeled vesicles near release sites. In addition, to determine if recycling vesicles matured into the main reserve cluster over time, the location of FM1-43-labeled vesicles was also examined in terminals that were fixed at a late time point following dye loading.

4.2 Materials and Methods

The preparation of animals, experimental setup and electrophysiology were done as reported in Chapter 2 – General Materials and Methods.

4.2.1 Photoconversion of FM1-43

To investigate the precise location of FM1-43-labeled vesicles in crayfish axon terminals, the FM1-43-dye was photoconverted into an electron dense precipitate. The photoconversion technique exploits the tendency for FM dyes to generate free radicals under intense illumination. The free radicals oxidize the chromogenic hydrogen donor 3,3'-diaminobenzidine (DAB) to produce a stable, insoluble, electron-dense precipitate that can be detected with transmission electron microscopy (Harata et al., 2001; Henkel et al., 1996; Sandell and Masland, 1988). DAB is only oxidized in the immediate vicinity

of the fluorescent molecules because the free radicals are short-lived (Harata et al., 2001). As a result, this technique ensures precise labeling of vesicles or endosomes containing FM1-43. Additionally, the proportion of photoconverted vesicles is relatively consistent through multiple sections of a nerve terminal (Harata et al., 2001).

FM1-43 loading, fixation, and washing

Because photoconversion of FM1-43 dye had not been reported for crayfish synapses prior to this study, the protocol was adapted from Denker et al. (2011a). After dye loading (3 min, 20 Hz stimulation of the excitor axon), the preparations were fixed with ice-cold 2.5% glutaraldehyde buffered solution (0.1 M phosphate buffer, 120 mM NaCl, pH 7.3) for 20 minutes on ice, followed by 20 minutes at room temperature. Preparations were then washed with buffered solution for 10 minutes followed by an ammonium chloride (100 mM in buffered solution) wash for 10 minutes to quench glutaraldehyde-induced autofluorescence. The preparations were washed again in buffered solution for 30 minutes (three 10-minute washes). All washing and quenching steps were performed at 4°C.

Photoconversion

The preparations were incubated in 1.5 mg/mL DAB (in crayfish buffered solution) at 4°C in the dark for 30-40 minutes. The DAB solution was then refreshed and FM1-43-labeled nerve terminals were illuminated with a 120W X-Cite 120 Q light (Lumen Dynamics, Mississauga, ON) through an Olympus LUMPlanFl/IR 40X/0.80 NA water objective until a dark precipitate appeared (15-20 minutes). The area of illumination was restricted to a diameter of ~100 μm by a field stop aperture. A modified filter set was used to excite the FM1-43 (470/40-nm excitation filter, 500-600 emission filter). After photoconversion, the preparations were rinsed in buffered solution for at least 5 minutes and stored in fixative at 4°C until TEM processing.

For a detailed protocol of the FM1-43 photoconversion process, including solutions, troubleshooting tips and TEM tissue processing and sectioning, see Appendix A.

Additionally, prior to photoconversion of FM1-43, we attempted two alternative labeling methods using horseradish peroxidase (HRP) and cationized ferritin (CF). The protocols and outcomes of those labeling methods are presented in Appendix B.

4.2.2 Transmission electron microscopy

Tissue processing

All preparations were micro-dissected in buffered solution to isolate single or small bundles of muscle fibers containing the terminals of interest. The dissected tissue was post-fixed with 1% osmium tetroxide in sodium cacodylate buffer (100 mM, pH 7.4) for 15 minutes and then washed in distilled water. The tissue was dehydrated in an ascending ethanol series (50%, 70%, 85%, 95%, 100% two times), immersed in a 50:50 mixture of Spurr's epoxy resin (Electron Microscopy Sciences, EMS) and 100% ethanol for 1 hour, and then in pure resin overnight. The following day the resin was replaced and the tissue infiltrated for an additional 4 hours. During this time, embedding molds (flat, rubber) were filled halfway with fresh, pure resin and partially polymerized at 70°C for 3.5 hours. The tissue was then placed on the surface of the partially polymerized resin and the upper portion of the molds were filled with resin and fully polymerized overnight at 70°C. This embedding method allowed the terminals and muscle fibers to be cut in cross section (see Appendix A).

Tissue sectioning and imaging

Thick sections (0.5 μm) were collected on glass slides, stained for 30 seconds at 60°C with 1% toluidine blue, washed with distilled water, and cover-slipped. Sections were examined by light microscopy (Nikon YS100) and photographed with an Olympus Q Color 3 digital camera.

For TEM, tissue blocks were trimmed and thin-sectioned (60-90 nm, silver interference colour) using an Ultra 45° Diatome diamond knife. Sections were cut in

series and collected on 1% parlodion-coated slotted grids. Sections were examined with a JEOL 1400 transmission electron microscope and imaged with a Gatan SC-1000 digital camera. Calibration of images was performed by imaging a carbon replica grid (0.463 μm spacing, Electron Microscopy Sciences) at the same magnifications for tissue observation.

4.2.3 Image analyses and statistical analyses

ImageJ software was used to measure the distribution of photoconverted, electron dense synaptic vesicles and vesicle diameter. To measure spatial distribution, images of serial sections (3-10 sections) were arranged in an image stack, and then the shortest distance to the nearest active zone was measured for each photoconverted vesicle using the straight-line tool in ImageJ (see Figure 14). Distributions of FM1-43-labeled vesicles were fit with nonlinear Gaussian distributions. The diameter of synaptic vesicles was also measured using the straight-line tool in ImageJ. Micrographs were overlaid with a grid pattern and sampled systematically. Synaptic vesicles were measured if the membranes were intact and not obscured by other organelles. Between 1312-2603 vesicles was used for diameter measurements. All values are reported as mean ±SEM. Significant differences of $P < 0.05$ were calculated using Prism 5 software. One-way ANOVAs were performed providing data met assumptions of equal variance (Fligner-Killeen test) and normality (Shapiro-Wilk normality test). Otherwise, a non-parametric Kruskal-Wallis was used.

4.3 Results

4.3.1 Anatomical and ultrastructural description of the crayfish opener NMJ

Crayfish axon terminals are located on the periphery of muscle fibers, often at the vertices of the fibers or between neighbouring fibers (Figure 12A). Axons terminate

adjacent to the main contractile portion of the muscle fiber and are surrounded by non-contractile extensions of the sarcoplasm (Jahromi and Atwood, 1967) and glial elements (Sherman and Atwood, 1972). Axon terminals are located underneath the basement membrane of the muscle (Figure 12B) and are found near muscle nuclei and muscle mitochondria (Harrington and Atwood, 1995). The two types of axons terminate in close proximity to each other (Figures 12B and 13A) and at some locations the inhibitor makes synaptic contacts with the excitor as a way of regulating tension development (Figure 13B; DeMill and Delaney, 2005).

The postsynaptic opener muscle is representative of a tonic crustacean muscle (reviewed by Atwood, 1976). The slow acting tonic fibers are characterized by a lesser developed T-tubule system, long sarcomeres (10-15 μm), and a high ratio of thin to thick myofilaments (Jahromi and Atwood, 1967). The tonic fibers of the opener muscle develop tension slowly in a graded fashion, which is ideal for postural and repetitive locomotory activity (reviewed by Atwood, 1976).

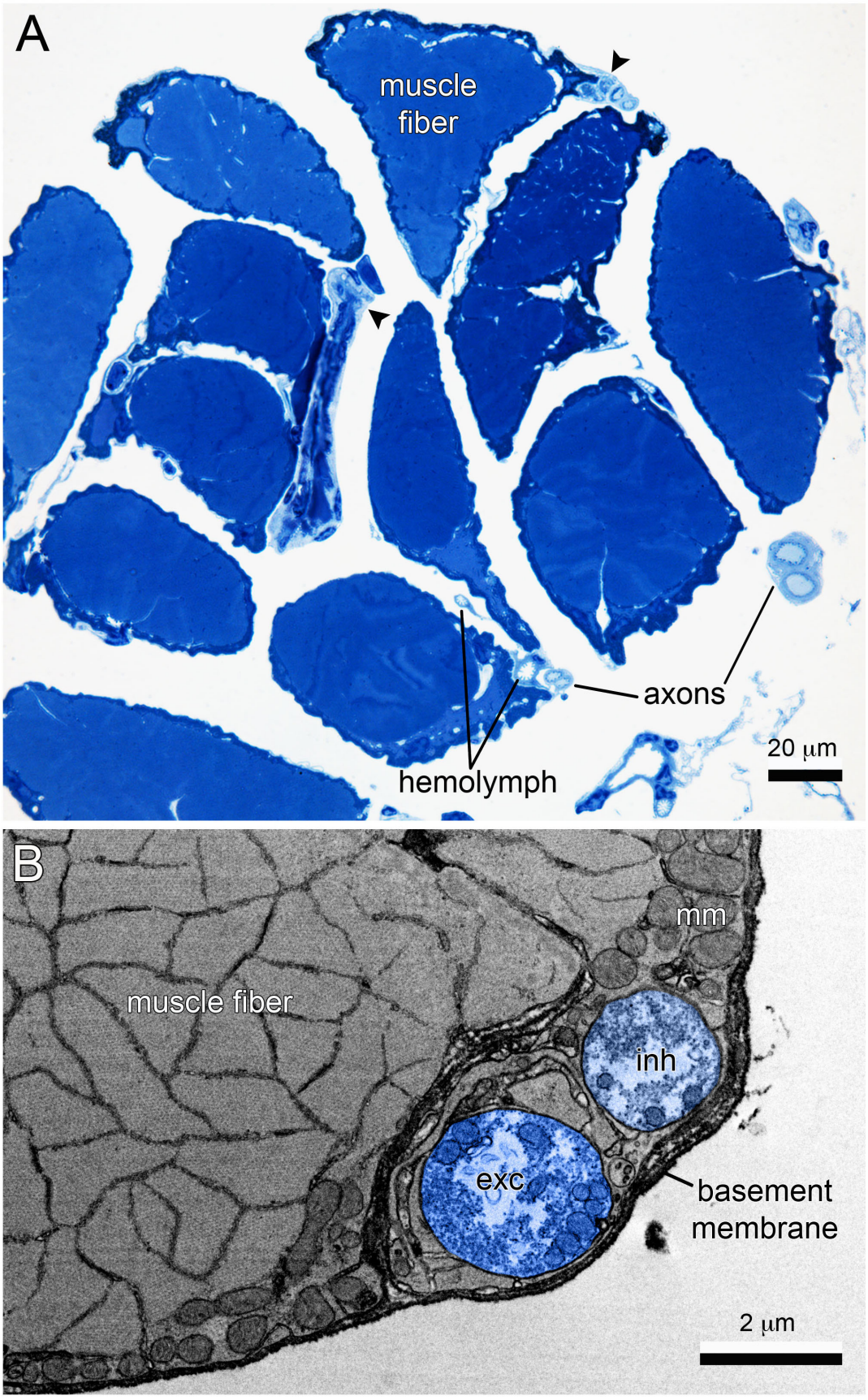
A
muscle fiber
axons
hemolymph
20 μm
B
mm
muscle fiber
inh
exc
basement membrane
2 μm

Figure 12. Association between axon terminals and opener muscle fibers. (A) Axon terminals are typically located on muscle fiber vertices and between neighbouring fibers (black arrowheads). Thick (0.5 μm) section stained with 1% toluidine blue, X60. (B) TEM showing inhibitory and excitatory axons (shaded blue) adjacent to one another at the periphery of a muscle fiber. The terminals are located underneath the muscle basement membrane and are surrounded by non-contractile extensions of the sarcoplasm and glial elements. Thin (60-80 nm) section stained with uranyl acetate, X10,000. exc: excitor axon terminal, inh: inhibitor axon terminal, mm: muscle mitochondria.

Crayfish axon terminals range in diameter from 1.5-10 μm and the connecting neck regions are approximately 0.5 μm in diameter (Florey and Cahill, 1982). The large and small terminals are referred to as main trunks and side branches, respectively (Jahromi and Atwood, 1974). The main trunks contain mitochondria, glycogen granules and clusters of neurotransmitter-containing vesicles clustered around numerous active zones (Figure 13; King et al., 1996), while the side branches are composed mostly of synaptic vesicles and contain few glycogen granules and mitochondria (Jahromi and Atwood, 1974). Synaptic vesicles are identified as small membrane-bound, clear-cored organelles with diameters between 40-45 nm (Sherman and Atwood, 1972). Glutamate-containing vesicles are spherical whereas GABA-containing vesicles are elongate (Figure 13B; Sherman and Atwood, 1972). Glycogen granules appear as 35-45 nm rosettes with uniform electron density when stained with heavy metals (Figure 13B).

Main nerve trunks contain several active zones, which are characterized by uniform separation of approximately 20 nm between pre- and postsynaptic membranes (Figure 13B; Jahromi and Atwood, 1974). A cluster of synaptic vesicles usually occupies the spaces behind the active zones. Active zones are the sites of synaptic vesicle fusion and are historically identified by their dense intramembranous entities, which are assumed to be P-type voltage-gated calcium and other ion channel proteins that are in close association with sites of vesicular fusion (Cooper et al., 1996; Heuser et al., 1974). The presence of morphologically docked, readily releasable vesicles along the length of the closely apposed presynaptic membrane is also an indication of a functional synapse

(Schikorski and Stevens, 2001). For the purpose of this thesis, the active zone will define both the sites of vesicle fusion (release sites) and the clusters of vesicles occupying the spaces behind the release sites.

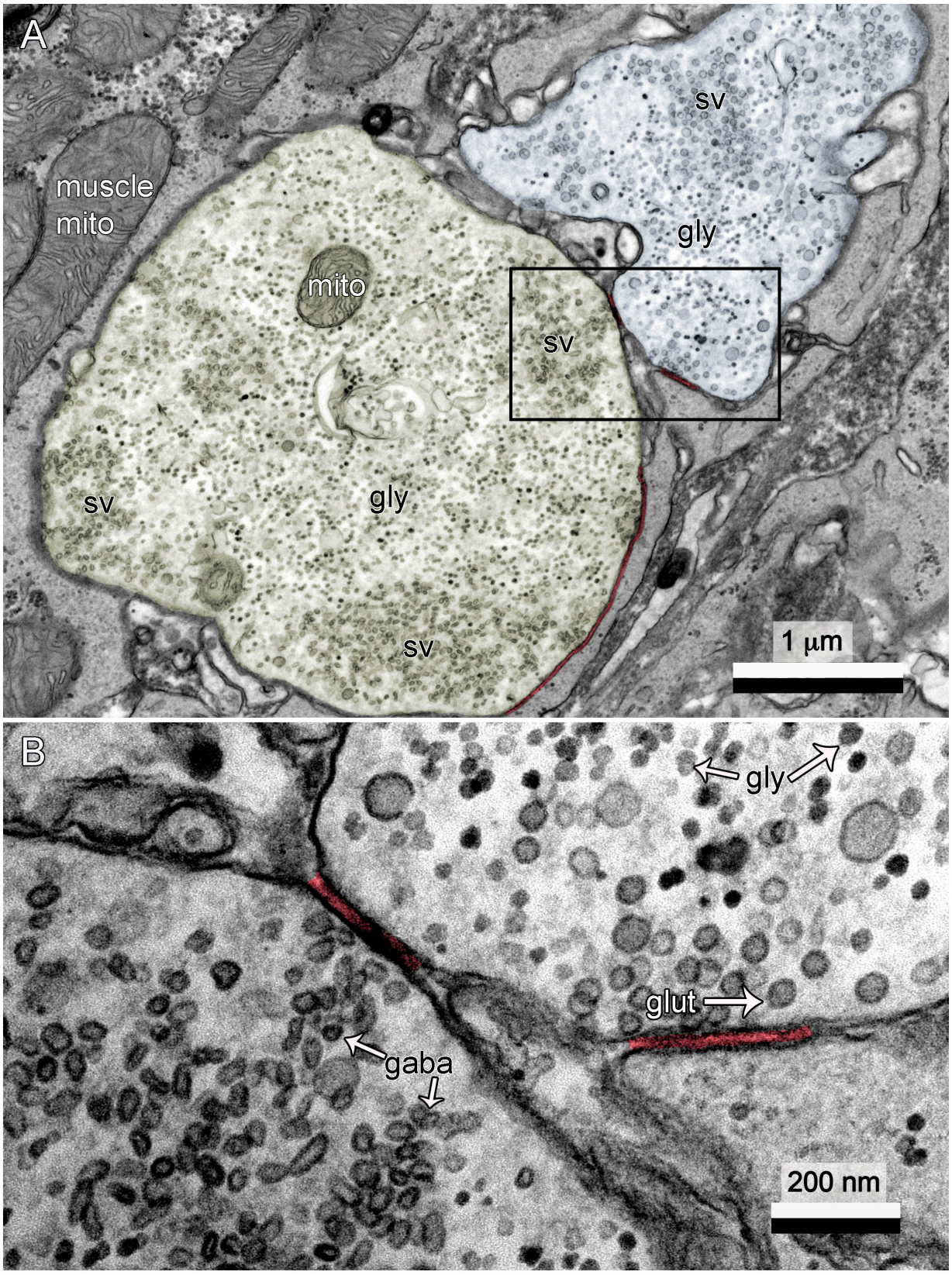
A
sv
muscle
mito
gly
mito
sv
sv
gly
sv
1 μm
B
gly
glut
gaba
200 nm

Figure 13. Presynaptic components of crayfish axon terminals. (A) Excitatory (blue) and inhibitory (yellow) terminals contain clusters of synaptic vesicles (sv), typically located near the plasma membrane. Mitochondria (mito) occupy the center and glycogen (gly) is dispersed throughout the terminal space. X20,000. (B) Enlarged region from A showing that inhibitory and excitatory terminals can be distinguished by the shape of their synaptic vesicles. Glutamate-containing vesicles (glut) are round and uniform whereas GABA-containing vesicles (gaba) are elongate and irregular. Synaptic vesicles cluster near release sites (red) and vesicles that are in contact with the presynaptic membrane at an active zone are considered docked and ready to exocytose. Glycogen granules occupy the space around vesicles and are distinguished by their rosette shape and, if the tissue is stained a certain way, their solid electron-dense appearance. X120,000.

4.3.2 Spatial distribution of FM1-43-labeled vesicles at early and late time points

To determine if recycling vesicles were spatially separated from reserve vesicles following endocytosis, the location of photoconverted vesicles was measured in relation to release sites (Figure 14). The location of electron dense vesicles in terminals that were fixed 2 minutes after stimulation were compared to terminals fixed 180 minutes after stimulation. The 2-minute condition represented the early time point where retention of vesicles near the release sites was expected (spatial separation). The 180-minute condition represented the late time point where intermixing of labeled vesicles with non-labeled vesicles in the vesicle cluster was expected (maturation).

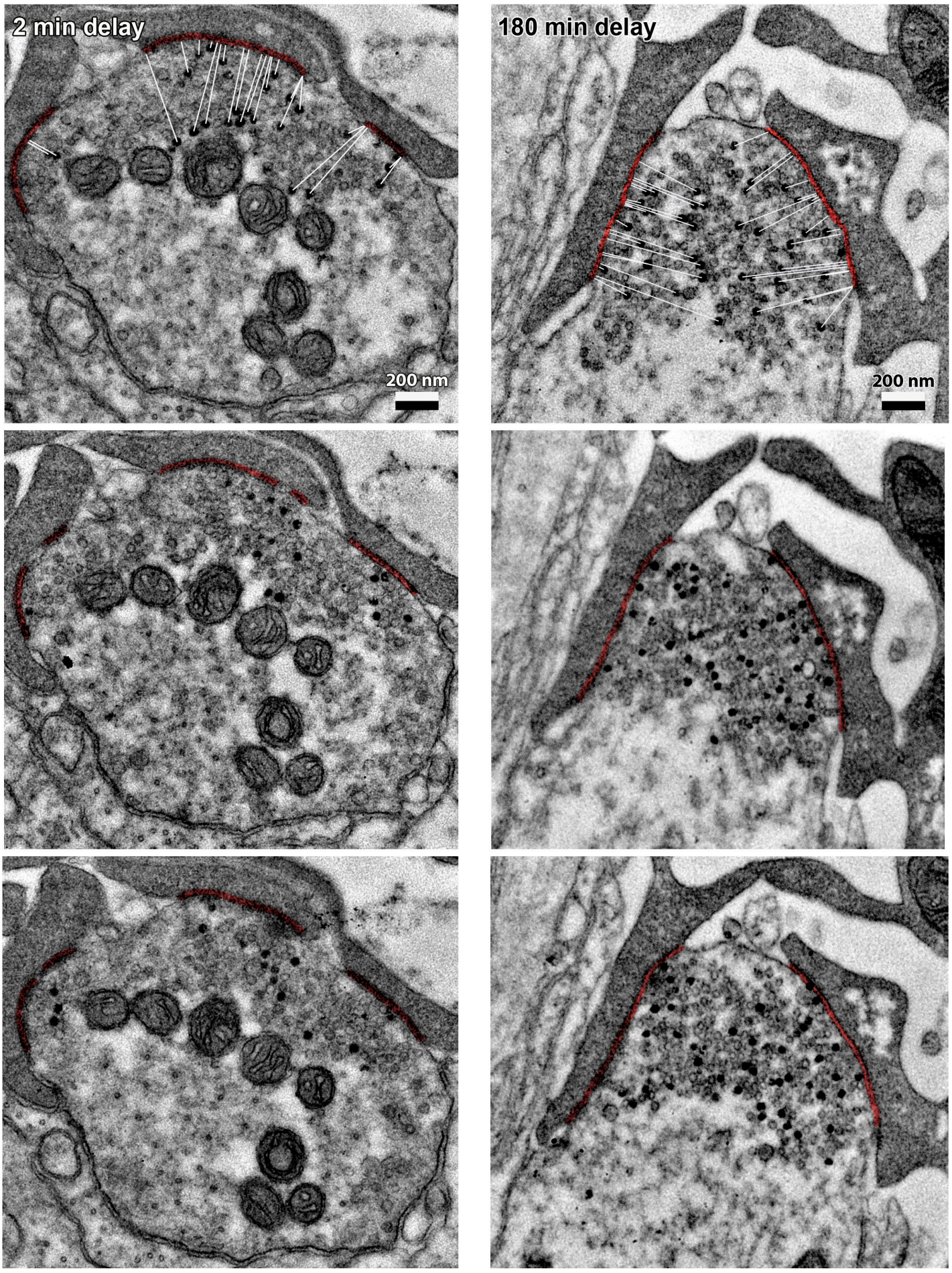
2 min delay
200 nm
180 min delay
200 nm

Figure 14. FM1-43-labeled vesicle distribution at early and late time points. The spatial distribution of FM1-43-labeled vesicles in 60-nm-thick serial sections of terminals fixed 2 minutes (left column) and 180 minutes (right column) following stimulation. The distribution of vesicles was measured by drawing a straight line (white line) from the center of the vesicles to the nearest part of the release sites (red). The FM1-43-labeled vesicles were easily distinguished by their electron dense lumens, compared to clear-cored unlabeled vesicles. The spatial distributions at early and late time points were similar. X40,000.

The spatial distribution of labeled vesicles was measured as the shortest straight-line distance to the nearest release site (Figure 14 and Figure 15). The distribution of vesicles was plotted for individual active zones fixed 2 minutes (7 active zones from 2 animals) and 180 minutes (8 active zones from 2 animals) following stimulation (Figure 15). Active zones were defined as clusters of vesicles corresponding to sites of vesicle release. Docked synaptic vesicles were defined as having centers 17-23 nm from the presynaptic membrane, based on classification from (Reist et al., 1998). The electron dense lumens of photoconverted synaptic vesicles were easily distinguished from the clear-cored non-photoconverted vesicles. The distances from the active zones were organized into 100 nm bins. Vesicles considered docked were placed at 0 nm, whereas vesicles not docked but within 100 nm were placed at 100 nm, and so on. The vertical dashed lines in Figure 15 indicate the farthest distance of any vesicle in the clusters from the release sites.

It was found that when tissue was fixed 2 minutes following stimulation, FM1-43-photoconverted vesicles showed no obvious retention near the release sites. The labeled vesicles were instead distributed throughout the total vesicle cluster. In addition, four of the seven active zones in the 2-minute condition had photoconverted vesicles located in the farthest bin, and all seven active zones had vesicles situated within 100 nm of the farthest bin. As with the early fixation condition, FM1-43-labeled vesicles were also found near the back of the vesicle clusters in the 180-minute active zones (typically within 100 nm of the farthest bin).

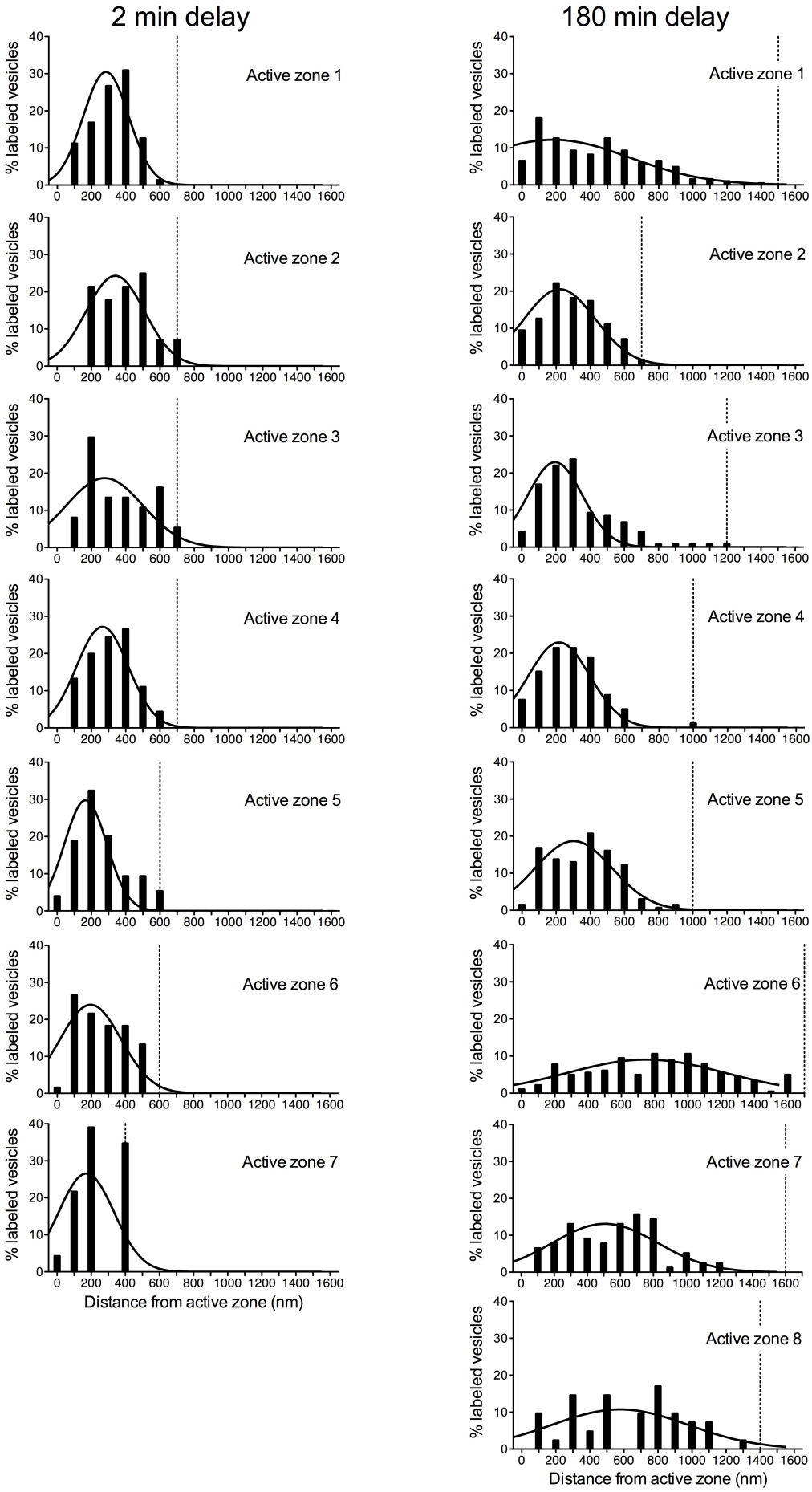
2 min delay
180 min delay
Active zone 1
Active zone 2
Active zone 3
Active zone 4
Active zone 5
Active zone 6
Active zone 7
Active zone 8
% labeled vesicles
Distance from active zone (nm)
0 200 400 600 800 1000 1200 1400 1600
0 10 20 30 40

Figure 15. Distribution of electron dense FM1-43-photoconverted synaptic vesicles relative to release sites. The percentage of labeled vesicles found docked (0 nm) or in 100 nm bins away from release sites is similar in early (2 minute, left column) and late (180 minute, right column) time points. Active zones include release sites and synaptic vesicle clusters. The data were fit with Gaussian distributions. The vertical dashed lines show the distance of farthest vesicle in the active zones. The data illustrate no obvious retention of FM1-43-photoconverted vesicles at early time points.

The distribution of FM1-43-labeled vesicles was comparable between the early and late fixation conditions. The photoconverted vesicles in active zones 2-5 in the 180-minute condition had similar distributions to all of the active zones in the 2-minute condition. The comparable distributions could be the result of similar vesicle cluster sizes; the 180-minute distributions that were different (active zones 1, 6-8) had substantially larger vesicle cluster sizes than the rest. Among the similar sized active zones, the largest proportions of FM1-43-labeled vesicles were situated 200-400 nm from the release sites. Furthermore, the means ±SEM of the Gaussian peaks for the similar sized active zones were not statistically different (2 minute: 292.7 ±24.8, N = 7; 180 minute: 283.9 ±23.6, N= 4; unpaired t-test, P = 0.82).

Active zones 1 and 6-8 in the 180-minute condition contained substantially more vesicles (larger cluster size) compared to the rest of the active zones. FM1-43-labeled vesicles were distributed throughout the entire clusters of vesicles. It was not possible to determine if FM1-43-labeled vesicles fixed 2 minutes after stimulation shared similar distributions in large vesicle clusters. The vesicle distributions in the larger sized active zones appeared more evenly spread throughout the cluster and had less obvious retention of vesicles at a specific distance from the release sites compared to the smaller sized active zones. A large variation of the mean Gaussian peaks with the larger sized active zones was found (mean ±SEM = 554.2 ±118.8, N = 4).

One difference between the early and late fixation conditions was the percentage of vesicles docked at the release sites. More FM1-43-labeled vesicles were docked in the

180-minute fixation condition compared to the 2-minute fixation condition. The percentages of docked vesicles in the 2-minute and 180-minute conditions were 1.48% and 4.19%, respectively. The differences in the percentage of docked vesicles could be a result of the small number of terminals sampled or due to variation in the release probabilities of active zones.

These data showed no retention of newly formed vesicles near release sites in crayfish opener terminals. Instead, FM1-43-labeled vesicles were dispersed throughout the main vesicle cluster, including the back of the cluster. The data also showed no clear difference in the distribution of FM1-43-labeled vesicles at early (2 minutes) and late (180 minutes) time points following stimulation.

4.3.2 Characterization of synaptic vesicles fixed 30 seconds after stimulation

The dispersion of photoconverted vesicles in the 2-minute condition suggested that either recycling vesicles disperse quickly, or alternatively that there was never retention of recycling vesicles near release sites after endocytosis. In order to determine which scenario was occurring, the distribution of vesicles in terminals fixed 30 seconds following stimulation was investigated.

Axon terminals fixed 30 seconds following stimulation showed substantial amounts of membrane turnover (Figures 16A, B and 17). In the five terminals sampled (from 2 legs), the synaptic vesicles were distributed throughout the entire terminals, in contrast to vesicles organized into tight vesicle clusters near active zones at the previous time points (Figure 16). In addition, the majority of the vesicle and plasma membranes appeared to have greater electron density 30 seconds after stimulation compared to the membranes from the other conditions. The basement membranes adjacent to the terminals were also spotted with electron densities, suggesting that the staining was from photoconverted FM1-43 that had not been rinsed away. The lumens of the majority of synaptic vesicles, however, were not electron dense. This type of staining had not been observed in the previous conditions. Due to both the lack of clustering near release sites and the absence

of FM1-43 staining in the vesicle lumens, the distribution of FM1-43-labeled vesicles at the 30-second time point could not be measured because it was not possible to identify which vesicles were properly stained.

A noticeable difference between the 30-second condition and the later fixation conditions was the diameter of the vesicles. The vesicles fixed 30 seconds after stimulation varied in diameter (Figure 16B), and most appeared bigger than the vesicles fixed 2- and 180-minutes after stimulation (Figure 16D, F). Specifically, a fraction of the 30-second vesicles were substantially larger and appeared to be more like endosome structures than functional vesicles (Figure 17). The largest vesicles were often found at the periphery of the vesicle cluster and were close, but not attached to, the plasma membrane (Figure 17D, E). In addition to the large vesicles, there was evidence of other endosome-like structures in the 30-second terminals (Figure 17A-C). The other structures appeared to be connected to the plasma membrane. One was comprised of smaller varicosities resembling synaptic vesicles, which were connected to each other by an electron dense membrane, forming a ring (Figure 17B). This type of organelle had previously been described as a ‘multivesicular body’ in crayfish axon terminals, implying the presence of multiple vesicles connected to one structure (Thompson and Atwood, 1984). The second structure was a deep, narrow invagination of the plasma membrane and appeared to have a vesicle budding from one end of it (Figure 17C).

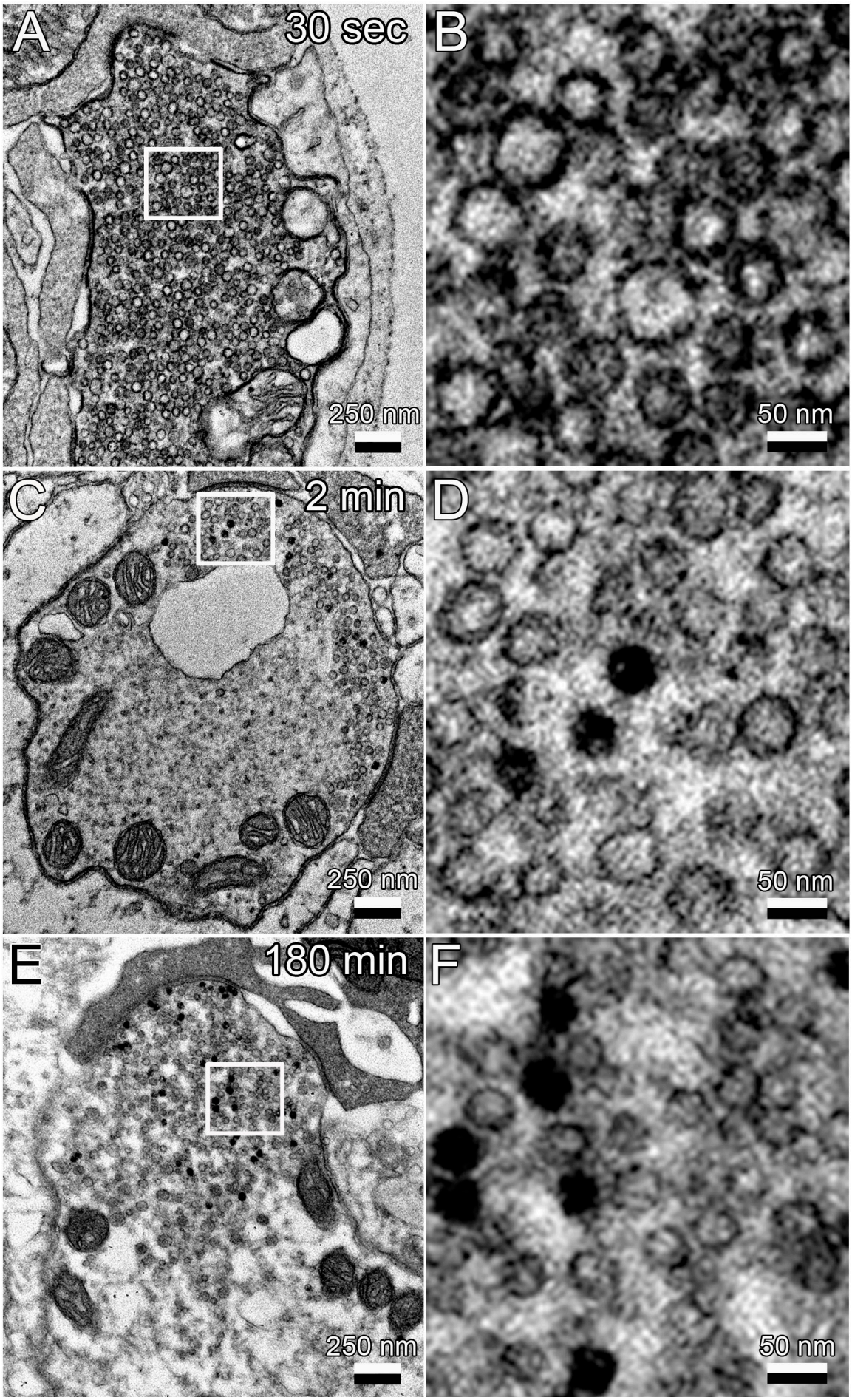
A
30 sec
250 nm
B
50 nm
C
2 min
250 nm
D
50 nm
E
180 min
250 nm
F
50 nm

Figure 16. Crayfish axon terminals turn over large amounts of membrane during 20-Hz stimulation. Axon terminals fixed 30 seconds following 20-Hz stimulation were filled with vesicles of varying sizes. The vesicles spanned the entire cytoplasmic area of the terminal instead of being clustered near release sites when compared to the 2 and 180 minute stimulations). Vesicles also appeared larger in diameter and showed greater membrane staining in the 30-second stimulation. By 2 minutes following stimulation, vesicles were redistributed and found clustered near release sites.

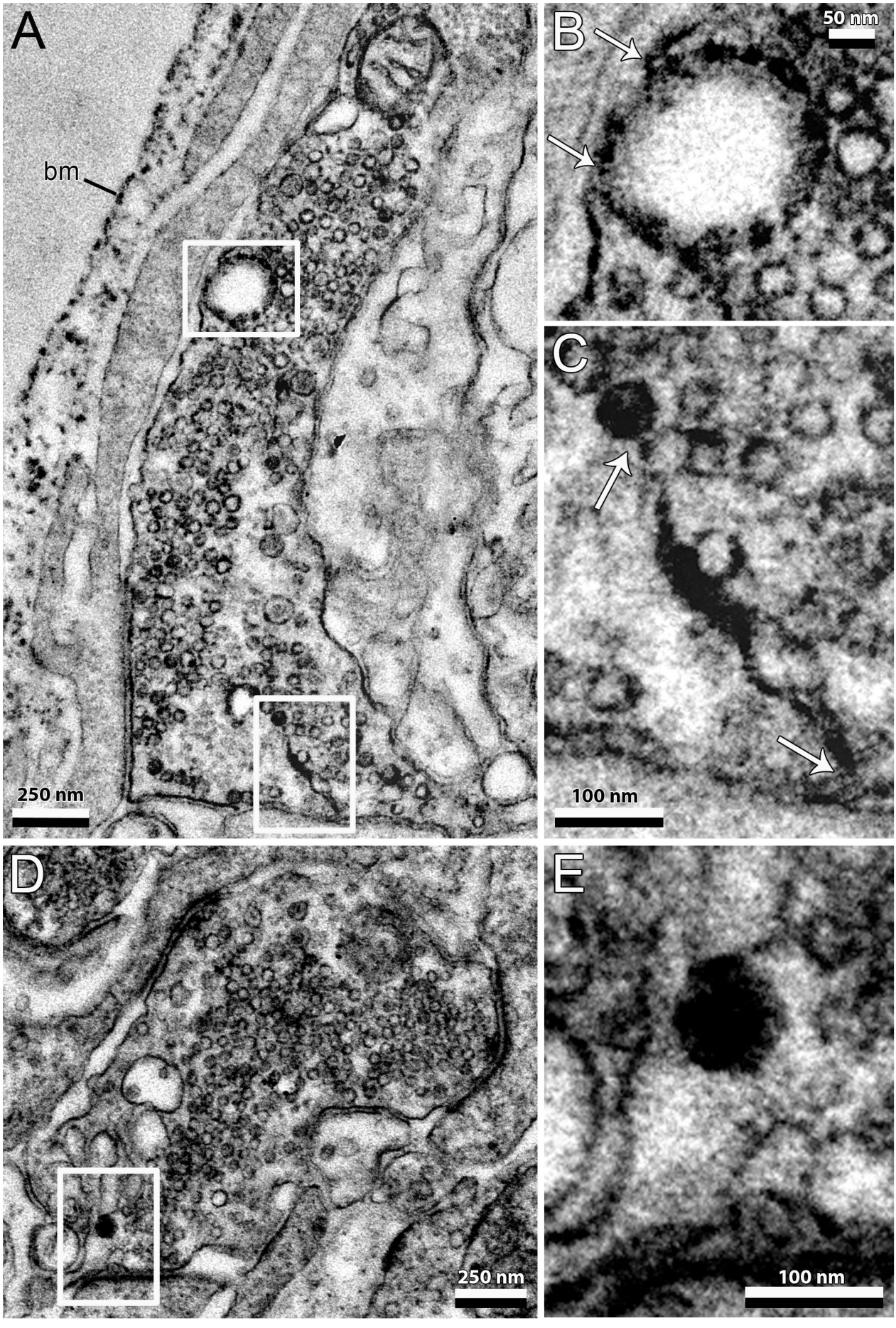
A
bm
250 nm
B
50 nm
C
100 nm
D
250 nm
E
100 nm

Figure 17. Terminals fixed 30 seconds following stimulation contain several endosome-like intermediates. (A) An axon terminal fixed 30 seconds after stimulation contained two distinct endosome-like structures (boxes). (B) The first organelle had the appearance of a multivesicular body and appeared to be connected to the plasma membrane (arrows). (C) The second structure was also connected to the plasma membrane (bottom arrow) but was a deep and narrow invagination. It appeared to have a vesicle budding from the tip (top arrow). (D) The terminals also contained large round vesicles (E). The large vesicles were found the most frequently out of the three endosome-like structures and varied greatly in diameter. The large vesicles were not connected to the plasma membrane but were located near it at the periphery of the vesicle cluster. bm: basement membrane.

The diameters of the vesicles in the 30-second conditions were measured to compare with vesicles from the 2- and 180-minute conditions (Figure 18). Vesicle diameters were plotted as frequency distributions with 5 nm bins and fit with nonlinear Gaussian distributions (Figure 18A). The mean ±SEM of vesicle diameters at 30 seconds, 2 minutes and 180 minutes following stimulation were 51.72 ±0.22 nm (N = 2603 vesicles), 47.57 ±0.28 nm (N = 1312 vesicles) and 43.71 ±0.19 nm (N = 2477 vesicles), respectively (Figure 18B). The mean diameters were statistically different among the three time points (Kruskal-Wallis one-way ANOVA, $P < 0.0001$, $N \geq 1312$ vesicles). The mean diameters were also plotted using active zones as independent measures (Figure 18C) and were also statistically different among all three times (one-way ANOVA, Tukey-Kramer post-test, $P = 0.0001$). The actives zones were measured from two animals per condition.

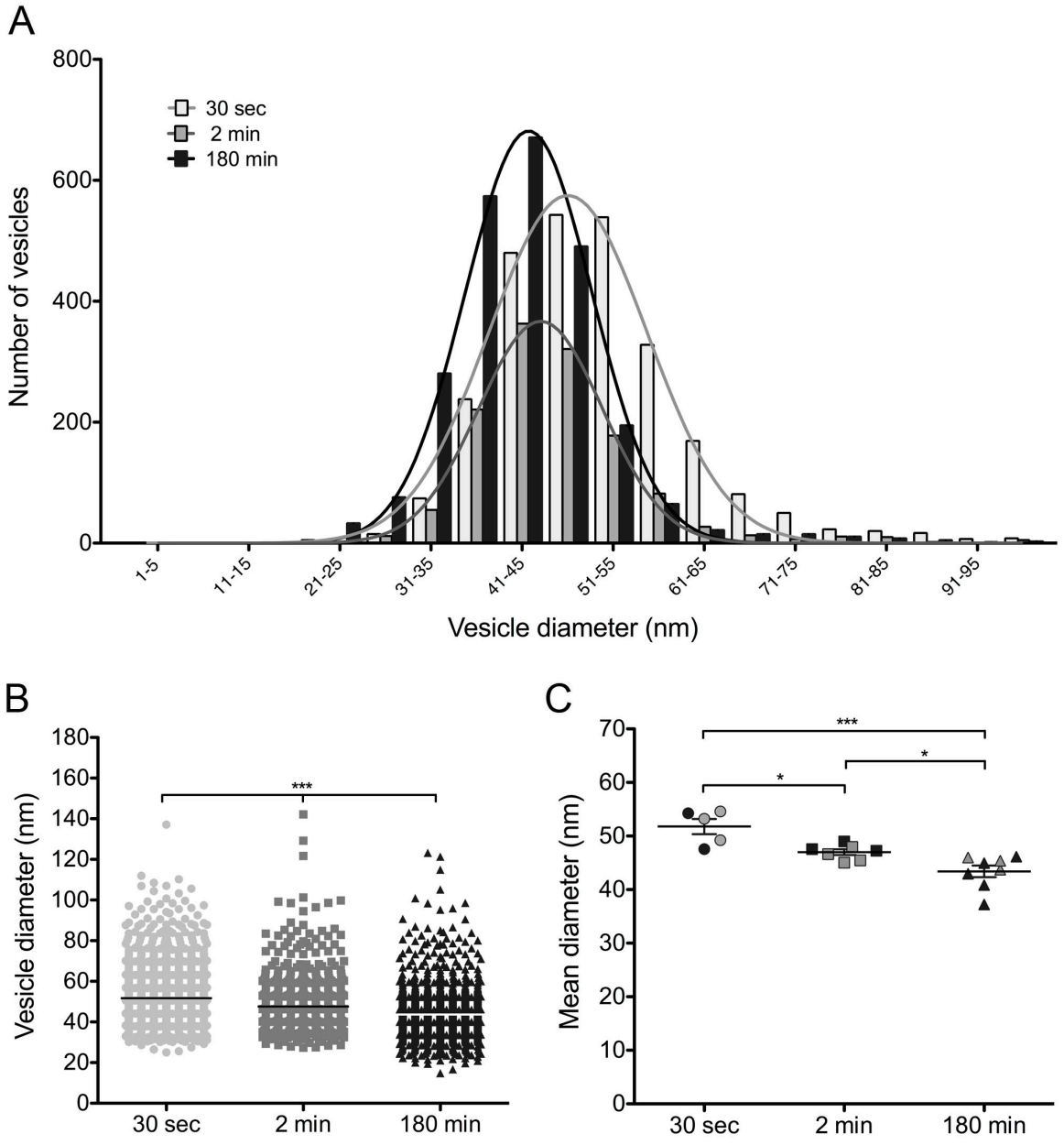

Figure 18. Axon terminals contain large vesicles 30 seconds after stimulation. (A) The frequency distributions of vesicle diameters show that vesicles are larger at 30 seconds post-stimulation compared to later time points. At 30 seconds following stimulation, vesicle frequency was greatest between 46-56 nm in diameter compared to 41-50 nm at 2 minutes and 36-46 nm at 180 minutes. The data were fit with Gaussian distributions. (B) The mean diameters of vesicles were statistically different among the three fixation times when vesicles were counted as independent measures (Kruskal-Wallis one-way ANOVA, ***P <0.0001, N ≥1312). (C) When active zones were used as

independent measures, the mean diameters of vesicles were also statistically different (one-way ANOVA, Tukey-Kramer post-test, *P ≤0.05, ***P ≤0.001). The active zones were sampled from two independent animals, which are differentiated by the grey and black colours.

The data illustrate that larger vesicles dominated 30 seconds after stimulation but shifted toward smaller diameters within minutes. The surface area of vesicles at 30 seconds (51.7 nm) was 8403 nm^2 ($4\pi r^2$), while the surface area of vesicles at 180 minutes (43.7 nm) was 6005 nm^2. The vesicles fixed 30 seconds after stimulation were on average ~1.4 times the size of vesicles fixed at 180 minutes. The increase in the average size at 30 seconds appears to be due to an increase in the number of vesicles with diameters >56 nm, corresponding to the numerous endosome-like structures (large vesicles) seen throughout the terminals. The percentage of vesicles >56 nm in diameter sampled in the 30-second condition was 27.1% compared to 10.5% sampled at 2 minutes and 5.9% sampled at 180 minutes. Furthermore, the mean ±SEM of the large vesicle diameters in the 30-second condition was 65.2 ±0.4 nm with a surface area of 13,355 nm^2, approximately 2.2 times the size of the average vesicles fixed 180 minutes later.

These data showed that crayfish axon terminals underwent enormous amounts of membrane turnover during sustained 20-Hz stimulation, but were able to redistribute membranes and vesicles within 2 minutes following stimulation. At 30 seconds following stimulation, axon terminals were crowded with synaptic vesicles, many of which were the equivalent of 2-5 regular vesicle sizes. Additional structures resembling endosomes were also observed less frequently.

4.4 Discussion

This chapter investigated the spatial distribution of FM1-43-labeled vesicles in relation to release sites at early and late time points following stimulation. The purpose of the study was to try to determine if recycling vesicles are retained near release sites

after endocytosis and whether recycling vesicles mature into the reserve vesicle cluster over time. Spatial separation of functional vesicle pools is thought to occur in some synapses (Paillart et al., 2003; Teng and Wilkinson, 2000) but not others (Denker et al., 2009; Rizzoli and Betz, 2004). Spatial separation of functional vesicle pools at the crayfish claw opener NMJ had not been investigated prior to this study and our results will contribute to the findings from other synapse models. In this chapter the distribution of vesicles within crayfish axon terminals was examined by photoconversion of FM1-43 and serial-section TEM. We found that vesicles containing photoconverted FM1-43 dye were not retained near release sites 2 minutes following stimulation compared to 180 minutes following stimulation. The overall distributions of photoconverted vesicles were also not different between early and late time points when the active zones were similarly sized. To determine if retention of recycling vesicles occurred earlier than 2 minutes, axon terminals fixed 30 seconds following stimulation were also examined. The terminals fixed 30 seconds following stimulation appeared to be in a state of membrane reorganization where vesicles were dispersed throughout the terminal space instead of clustered near release sites. A large proportion of vesicles fixed 30 seconds following stimulation were larger in diameter than vesicles fixed 2 and 180 minutes following stimulation. Furthermore, the terminals fixed 30 seconds following stimulation contained numerous structures resembling endosomes (Richards et al., 2000; Watanabe et al., 2013a,b; Watanabe et al. 2014). Most of the structures were large round vesicles that would be comparable to fusion of 2-5 vesicles and were found detached from, but close to, the plasma membrane. The other endosome-like organelles had markedly different structures, suggesting that membrane retrieval might take multiple routes at this synapse.

4.4.1 Crayfish axon terminals undergo rapid redistribution of membranes during 20 Hz stimulation

These data showed that crayfish axon terminals recycle substantial amounts of membrane in response to continuous 20-Hz stimulation. The axon terminals that received 3 minutes of stimulation were entirely filled with vesicle-shaped organelles by 30 seconds following stimulation. The distribution of vesicles at 2 minutes following

stimulation, however, was remarkably different. By 2 minutes, synaptic vesicles were organized into distinct clusters behind vesicle release sites at the periphery of the terminal space and the centers of the terminals were no longer occupied with vesicles. The data showed that endocytosis and vesicle sorting occurs <2 minutes after sustained stimulation. This result is in agreement with similar experiments conducted on different synapse models. At the frog NMJ, fast modes of endocytosis were reported to occur <2 minutes after 30-Hz stimulation, as determined by FM2-10 unloading (Richards et al., 2000). An additional study used high KCl depolarization of cultured hippocampal neurons and FM1-43 labeling and found that endocytosis had a half-life of ~60 seconds and that once internalized, vesicles become release competent by ~30 seconds (Ryan et al., 1993). The time course of endocytosis was also estimated using quick-freeze electron microscopy techniques and involved counting the appearance of membrane invaginations (Miller and Heuser, 1984). The study determined that membrane invaginations reached a maximum at ~30 seconds and finished by ~90 seconds. These findings illustrate that endocytosis occurs in <2 minutes when preparations receive moderate to high frequency stimulations.

The spatial distribution of the FM1-43-labeled vesicles in axon terminals fixed 2 minutes after stimulation is no longer surprising given the dynamics of membrane turnover observed 30 seconds following stimulation. The terminals appeared to be in a state of reorganization after stimulation, with vesicle intermediates dispersed entirely throughout the terminal space. Assuming that the vesicles in the 30-second terminals were all formed during (and after) the stimulation, any photoconverted vesicles would be randomly dispersed throughout the terminal space. Therefore, the retention of FM1-43-labeled vesicles near release sites would not be expected once the vesicles were sorted into clusters 2 minutes following stimulation. It is worth questioning where a proportion of the internalized membrane went between 30 seconds and 2 minutes following stimulation, as there appeared to be more membrane inside the terminals at 30 seconds compared to 2 minutes. We suggest that some of the vesicle membrane is transported out of the axon terminals. Synaptic vesicles have been shown to move between terminals in cultured rat hippocampal neurons in an actin-dependent manner (Darcy et al., 2006;

Kamin et al., 2010; Westphal et al., 2008) and also in acute hippocampal slices (Staras et al., 2010). The movement of vesicles between terminals allows for constitutive sharing of vesicles and eliminates the need for terminals to autonomously replenish vesicle populations.

A notable difference in these findings was the enhanced contrast of both vesicle and plasma membranes in the 30-second condition compared to the 2- and 180-minute conditions. The membranes of the vesicles and axon terminals appeared to be more electron dense at 30 seconds following stimulation (see Figure 16). There was, however, an absence of reaction product in the majority of the synaptic vesicle lumens. The lack of lumenal staining should not be caused by the larger diameters of the vesicles because fully stained large vesicles were observed (see Figure 17). The enhanced contrast was presumably caused by FM1-43 photooxidation of DAB since no additional heavy metal staining was performed in the 30-second condition compared to the others and there is also no endogenous peroxidase activity in synaptic vesicles to cause precipitation of DAB (Henkel et al., 1996). The 30-second preparations also showed scattering of electron dense specs in the basement membranes adjacent to terminals, resembling FM1-43 molecules that had likely not been washed from the extracellular membranes. This form of photoconversion staining has not been previously described and could be an artifact of the early fixation time.

This thesis is the first to illustrate the vast amount of membrane recycling in response to continuous 20-Hz stimulation at the crayfish opener NMJ. The data has demonstrated that under continuous 20-Hz stimulation, recycling of synaptic vesicles can occur in <2 minutes. Specifically, crayfish axon terminals contain many vesicle intermediates 30 seconds after stimulation and are able to redistribute and organize the vesicles into clusters near release sites by 2 minutes.

4.4.2 Putative endosomes in crayfish terminals are large vesicles

The ultrastructural data showed the presence of large vesicles in crayfish axon terminals 30 seconds following stimulation. It is proposed that these large vesicles are the primary endosomes in this synapse. Large vesicles have been reported in crayfish opener axon terminals (Thompson and Atwood, 1984); however, the large vesicles were thought to be a product of the experimental technique, where low temperatures (4°C) might have increased membrane viscosity and altered kinetics of membrane retrieval. There is also morphological evidence of large round vesicles in crayfish abdominal extensor synapses (Jahromi and Atwood, 1967), and leg extensor synapses (King et al., 1996) but the structures were never discussed. Interestingly, large vesicles have recently been reported in *C. elegans* NMJs (Watanabe et al., 2013a) and mouse hippocampal synapses (Schikorski, 2014; Watanabe et al., 2013b). The large vesicles described by Watanabe *et al*. (2013a,b) were formed in response to single release events and formed as quickly as 50-100 ms following stimulation ('flash-and-freeze' method). They were formed in peri-active regions via large invaginations of the plasma membrane and were ~82 nm in diameter (~4 vesicle sizes). In a follow-up study, Watanabe et al. tracked the fate of the large vesicles with subsequent fixation time points using the same high-pressure freezing technique (Watanabe et al., 2014). They discovered the presence of even larger round organelles (~116 nm, or 8 vesicle equivalents) a short time after the large vesicles were formed, suggesting that the large vesicles fuse with each other to form synaptic endosomes. They also showed synaptic vesicles budding off of the endosome structures at later time points, providing evidence for the functionality of the endosomes. The study by Schikorski (2014) also reported large vesicles on the timescale of 10-40 seconds following stimulation. Schikorski briefly stimulated cultured neurons (20 Hz for 2 seconds) in the presence of FM1-43 and performed photoconversion electron microscopy at various time points. He observed the emergence of large FM1-43-labeled vesicles (up to 4 vesicle sizes) 10 seconds following stimulation. The large vesicles dominated in relation to other FM1-43-labeled vesicles at 20 seconds following stimulation and were located around the main vesicle cluster. After 20 seconds, the fraction of large vesicles decreased until 90% of labeled vesicles were single sized at 40 seconds following

stimulation. Based on Watanabe et al. (2014) we suggest that Schikorski's shift towards a smaller vesicle size over time occurs as synaptic vesicles bud from the large vesicle. At 30 seconds following stimulation, the terminals in our study contained a range of large vesicle sizes (2-5 vesicle equivalents), and importantly, not all of the vesicles measured were formed 30 seconds following stimulation because many of the vesicles would have formed during the loading stimulus. Therefore, because the loading stimulus was so long it is more accurate to assume that the terminals fixed 30 seconds following stimulation were snapshots of vesicle formation over 3.5 minutes with the majority of vesicles formed during the loading stimulus. Interestingly, the terminals contained a range of large vesicles but the highest proportion had smaller diameters (e.g. 2 vesicle sizes) and the lowest proportion had larger diameters (e.g. 5 vesicle sizes). We propose that the majority of the large vesicles had smaller diameters because they had formed during the loading stimulus and thus had more time to bud vesicles, leading to a reduction in their size. In contrast, a smaller proportion of the large vesicles had bigger diameters because they had formed at the end, or after, the loading stimulus and had less time to produce functional vesicles via budding. Lastly, if the large vesicles in our preparations fused together to form endosomes (similar to Watanabe et al., 2014), it is likely that those events happened by the time our terminals were fixed.

The 30-second data also showed evidence of other endosome-like structures, including a multivesicular body and a second organelle that appeared as a long, narrow membrane invagination with a budding vesicle (Figure 17). The two structures contained photoconversion reaction product and therefore were formed during FM1-43 incubation and the loading stimulation. The multivesicular body resembled a structure previously seen in the crayfish opener axon that had been fixed immediately following stimulation (Thompson and Atwood, 1984). The second structure appeared as a long invagination of the plasma membrane, similar to organelles reported at frog NMJs (Richards et al., 2000), snake motor terminals (Teng and Wilkinson, 2000), goldfish bipolar cells (Paillart et al., 2003), rat hippocampal neurons (Takei et al., 1996) and lamprey reticulospinal synapses (Gad et al., 1998). Both of the structures found in the terminals were seen only once and thus might represent alternative, less common recycling routes.

The data showed that at least three putative endosome structures form in response to sustained 20-Hz stimulation in crayfish claw opener axon terminals. The large round vesicles were observed most frequently and bear a strong resemblance to recently reported endosomes. The other endosome-like organelles appeared as bulk invaginations of the plasma membrane and multivesicular bodies. The appearance of multiple endocytic organelles implies that more than one route of vesicle recycling occurs at this synapse. This study can be seen as the first step in characterizing endocytosis, including potentially different endocytic routes, in crayfish motor neurons.

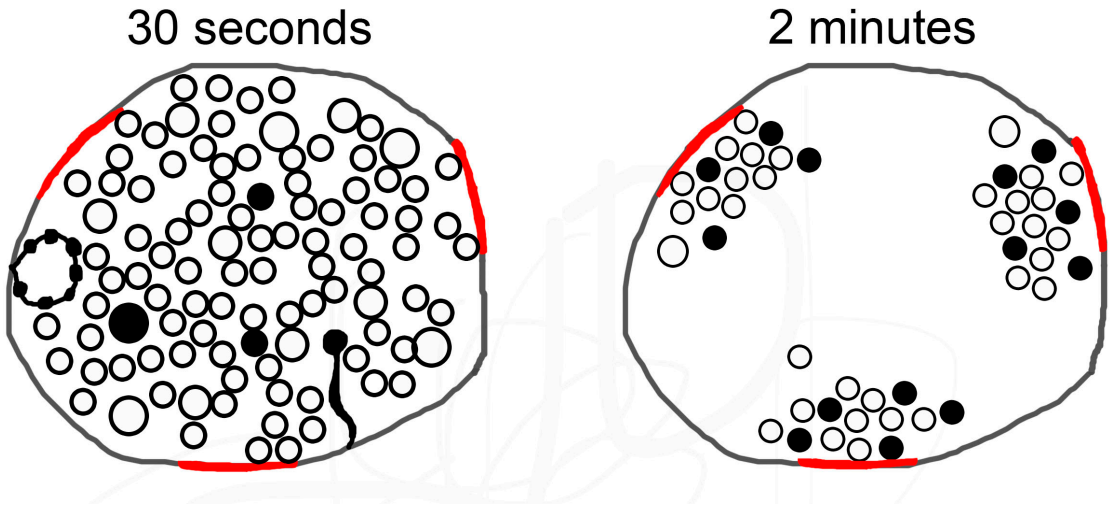

Figure 19. Schematic of synaptic vesicle recycling at the crayfish NMJ. Crayfish opener axon terminals recycle large amounts of membrane in response to continuous 20-Hz stimulation. At 30 seconds following stimulation, axon terminals are filled with vesicles of varying sizes and contain morphologically distinct endosome structures, suggesting multiple routes of endocytosis. The most commonly observed endosome-like structure is the large vesicle. By 2 minutes following stimulation, crayfish terminals have redistributed synaptic vesicles so that they are found clustered near release sites (red). Most of the vesicles are uniform in diameter, but several large vesicles also remain at the periphery of the clusters.

Chapter 5 – Conclusions and Future Directions

5.1 Does serotonin recruit vesicles from the reserve pool?

The results from the FM1-43 unloading experiments in Chapter 3 did not resolve a population of vesicles activated (and de-activated) by serotonin. Based on an FM1-43 unloading experiment conducted by Wang and Zucker (1998), it was hypothesized that serotonin recruits reserve vesicles during stimulation and then upon removal of serotonin, recruited vesicles return to their reserve state. The FM1-43 unloading experiment was unable to resolve serotonin-activated populations of synaptic vesicles however, and we suggest that FM1-43 imaging techniques are not ideal for determining effects of serotonin.

The hypothesis that serotonin recruits vesicles from the reserve pool has recently been investigated at the crayfish opener NMJ (Wu and Cooper, 2012) and the crayfish abdominal extensor NMJs (Wu and Cooper, 2013). In both studies, Wu and Cooper used bafilomycin A1, a vacuolar ATPase blocker, to perturb the repackaging of vesicles with glutamate during recycling. The authors applied continuous 20-Hz stimulation under the assumption that only the recycling pool would recycle at this frequency. Then when neurotransmission eventually depressed because recycling vesicles could not refill with glutamate, the authors applied serotonin and found partial and brief recovery of neurotransmission. They concluded that reserve pool recruitment was able to rescue neurotransmission. However, estimates of vesicle pool sizes in other synapse models suggest that the recycling pool comprises 20% of the total pool while the reserve pool contains the remaining 80% (Delgado et al., 2000; Harata et al., 2001; Richards et al., 2000; Richards et al., 2003; Rizzoli and Betz, 2004). If this were also true for crayfish synapses then the rescue by serotonin would result in significantly more neurotransmission for a longer period of time. Wu and Cooper further assumed that 20-Hz stimulation would only involve the recycling pool and our TEM data suggests that many, if not all, vesicles are recycled with continuous stimulation at 20-Hz frequency. It

is possible, however, that the recycling pool is larger than previously estimated at crayfish synapses, and thus the reserve pool is smaller. If this were so, recruitment of reserve vesicles would not significantly increase neurotransmission in Wu and Cooper's studies. Our TEM data at 30 seconds following stimulation does not reject this hypothesis, and although the terminals appeared to be in a state of abundant membrane turnover, it is possible that some vesicles remained immobile and non-releasable.

5.2 Where in the axon terminal is the unloadable FM1-43 in the 180-minute condition?

In crayfish preparations rested for 180 minutes following the FM1-43 loading stimulus, ~23% of dye could not be unloaded during the subsequent 50 minute unloading stimulus. It is possible that the inability to unload the FM1-43 dye from the terminals could be due to fusion of vesicular membranes into non-vesicular membranes. This is unlikely, however, because no obvious differences in the contrast staining of the very few non-vesicular organelles in the 180-minute TEM preparations were observed, suggesting that the non-releasable FM1-43 molecules are still associated with synaptic vesicles. We therefore maintain that the unloadable fluorescence in the 180-minute condition is located in non-releasable reserve vesicles. In light of the vast amounts of membrane turned over in the 30-second TEM data, however, it is perplexing that some reserve vesicles would not be recruited to release transmitter during 50 minutes of sustained 20-Hz stimulation. One way to verify that non-releasable FM1-43 dye remains inside non-releasable reserve vesicles would be to perform photoconversion electron microscopy on terminals that were loaded in FM1-43-containing solution, rested for 180 minutes, and then unloaded for 50 minutes in dye-free solution. The presence of reaction product in synaptic vesicles would confirm that some reserve vesicles are not recruited, even under sustained depolarization of axon terminals.

5.3 Synaptic vesicle pool localization in the crayfish NMJ: TEM data does not support FM1-43 unloading hypothesis

The similar vesicle distributions in the 2- and 180-minute conditions in Chapter 4 are unsurprising in light of the 30-second TEM data. The distributions are surprising, however, compared with the FM1-43 unloading data from Chapter 3. The unloading experiments in Chapter 3 and the TEM experiments in Chapter 4 had identical stimulation protocols and the same late time point (180 minutes). The data from the FM1-43 unloading experiments suggested that vesicles were more easily released 30 minutes after stimulation compared to 180 minutes; however, the TEM data showed no difference in distributions at early and late time points following stimulation. Excluding the unlikely possibility that synaptic vesicles position themselves closer to release sites around 30 minutes following stimulation, we suggest that functionality of vesicles does not depend on position in the active zone. Instead of position, the defining characteristics of recycling and reserve vesicles could be their biochemical markers like soluble vesicle-associated proteins. For example, newly formed vesicles might have few soluble tethering proteins like synapsins associated with their membranes and, thus, would not readily adhere to other vesicles. Over time, however, the vesicles could slowly accumulate synapsin proteins as they freely diffuse around the terminal space (Denker et al., 2011). Recycling vesicles that have accumulated a small number of synapsins could link to the periphery of the main reserve cluster. The link might be weak, however, and the vesicles could probably untether from the cluster through phosphorylation by calcium-calmodulin-dependent kinases (CaM kinases) in response to brief activity-induced increases in intracellular [Ca^{2+}] (Benfenati et al., 1989; Hosaka et al., 1999; Sihra et al., 1989). Maturation of recycling vesicles would eventually occur when the vesicles accumulated enough protein tethers to strongly connect them with the main reserve cluster and prevent them from untethering during depolarization.

The discrepancy between our FM1-43 imaging and photoconversion TEM experiments is supported by previous studies. Early reports at the *Drosophila* NMJ suggested a spatial separation of functional vesicle pools with FM1-43 imaging (Kuromi

and Kidokoro, 1998; Kuromi and Kidokoro, 1999; Kuromi and Kidokoro, 2000; Kuromi and Kidokoro, 2002; Kuromi et al., 2004). However, when the hypothesis was tested with electron microscopy, complete intermixing between recycling and reserve vesicles was observed (Denker et al., 2009). A separate study also recently examined *in vivo* recycling of synaptic vesicles in 10 different animal models using photoconversion of FM1-43 and serial electron microscopy (Denker et al., 2011). The study determined that only a small percentage of vesicles recycle in vivo (~5%) and that the distribution of the recycling vesicles is not localized near release sites. Crayfish synapses were not included in the Denker et al. (2011a) study and so although spatial separation of functional vesicle pools in our preparation seems unlikely, the hypothesis can still be tested. Future studies aimed at testing whether recycling vesicles are retained near release sites could be done with two modifications: brief stimulations and short delays after stimulation. An experimental design might include fast fixation methods like microwave-assisted fixation (Schikorski, 2014) or rapid high-pressure freezing (Watanabe et al., 2013a,b) to capture the location of recycling vesicles <1 second after endocytosis.

5.3.1 Future studies to look at membrane redistribution

In order to understand how crayfish axons reorganize membranes in response to 20-Hz stimulation, subsequent time points should be added to this experiment. To do so, axon terminals should be fixed and photoconverted at short time intervals between 0 seconds and 2 minutes (e.g. 15 second intervals). This approach would provide a better understanding of how the terminals redistribute vesicle membranes, but it would be labour intensive. An alternative experiment would be to monitor the axon terminals during and after stimulation via high-resolution fluorescence imaging techniques (e.g. 2-photon). If clusters of vesicles are being transported out of axon terminals for use elsewhere (Darcy et al., 2006; Kamin et al., 2010; Westphal et al., 2008), lumps of fluorescence should be seen moving out of terminals. In fact, our laboratory has seen retrograde movement of FM1-43 clusters out of crayfish axon terminals ~10 minutes following stimulation. Membrane dynamics will need to be examined at earlier time points than 10 minutes, however. This research will add to previous work in cultured

neurons and hippocampal slices to illustrate dynamic movements of vesicle clusters between axon terminals.

5.4 Large vesicles might function as endosomes in the crayfish NMJ

As discussed in 4.4.2, large vesicles were found in crayfish axon terminals and may function as endosomes. This thesis is the first attempt to describe the large vesicles found in crayfish axon terminals and to relate the structures to recent findings in cultured neurons (Schikorski, 2014; Watanabe et al., 2013b; Watanabe et al., 2014) and *C. elegans* NMJs (Watanabe et al., 2013a).

Future studies are required to reveal the function of large vesicles in crayfish synapses. The next experiments should determine if large vesicles exist in crayfish synapses under physiological conditions and whether they play a functional role in vesicle recycling. Paired impulses have been shown to occur in the claw opener excitor motor neuron of freely behaving crayfish (Wilson and Davis, 1965), so the experimental design should involve TEM on terminals that receive paired pulses and a very short delay before fixation (as discussed in 5.3). For a better understanding of whether large vesicles function as endosomes, and to determine the fate of the large vesicles, crayfish terminals should be fixed and analyzed over a period of time. A time series would provide information about how the large vesicles form (e.g. through bulk invagination of the plasma membrane or homotypic fusion of single vesicles), whether they fuse to form larger synaptic endosomes (Watanabe et al., 2014), and whether they bud synaptic vesicles. These studies would contribute to the emerging large vesicle component of vesicle recycling research (Schikorski, 2014; Watanabe et al., 2013a,b; Watanabe et al., 2014).

Bibliography

Abràmoff D, Magalhaes PJ, Ram SJ (2004) Image processing with ImageJ. Biophotonics International 11:36-42.

Atwood HL (1976) Organization and synaptic physiology of crustacean neuromuscular systems. Prog Neurobiol 7:291.

Ayali A, Harris-Warrick RM (1999) Monoamine control of the pacemaker kernel and cycle frequency in the lobster pyloric network. J Neurosci 19:6712-6722.

Azmitia EC (2001) Modern views on an ancient chemical: serotonin effects on cell proliferation, maturation, and apoptosis. Brain Res Bull 56:413-424.

Bazemore AW, Elliott KAC, Florey E (1957) Isolation of Factor I. J Neurochem 1:334-339.

Beltz BS, Kravitz EA (1983) Mapping of serotonin-like immunoreactivity in the lobster nervous system. J Neurosci 3:585-602.

Benfenati F, Bähler M, Jahn R, Greengard P (1989) Interactions of synapsin I with small synaptic vesicles: distinct sites in synapsin I bind to vesicle phospholipids and vesicle proteins. J Cell Biol 108:1863-1872.

Betz WJ, Mao F, Bewick GS (1992) Activity-dependent fluorescent staining and destaining of living vertebrate motor nerve terminals. J Neurosci 12:363-375.

Bittner GD (1968) Differentiation of nerve terminals in the crayfish opener muscle and its functional significance. J Gen Physiol 51:731-758.

Borst, JGG, Sakmann B (1996) Calcium influx and transmitter release in a fast CNS synapse. Nature 383:431-434.

Bunin MA, Wightman RM (1999) Paracrine neurotransmission in the CNS: involvement of 5-HT. Trends Neurosci 22:377-382.

Catterall WA, Few AP (2008) Calcium channel regulation and presynaptic plasticity. Neuron 59:882-901.

Ceccaldi P, Grohovaz F, Chieregatti E, Greengard P, Valtorta (1995) Dephosphorylated synapsin I anchors synaptic vesicles to actin cytoskeleton: an analysis by videomicroscopy. J Cell Biol 128:905-912.

Cesca F, Baldelli P, Valtorta F, Benfenati F (2010) The synapsins: key actors of synapse function and plasticity. Prog Neurobiol 91:313-348.

Cooper RL, Harrington CC, Marin L, Atwood HL (1996) Quantal release at visualized terminals of a crayfish motor axon: intraterminal and regional differences. J Comp Neurol 375:583-600.

Cooper RL, Hampson DR, Atwood HL (1995) Synaptotagmin-like expression in the motor nerve terminals of crayfish. Brain Res 703:214-216.

Danon D, Goldstein L, Marikovsky Y, Skutelsky E (1972) Use of cationized ferritin as a label of negative charges on cell surfaces. J Ultrastruct Res 38:500-510.

Darcy KJ, Staras, Collinson LM, Goda (2006) Constitutive sharing of recycling synaptic vesicles between presynaptic boutons. Nat Neurosci 9:315-321.

Delaney KR, Tank DW (1991) Calcium-dependent and calcium-independent enhancement of transmitter release at the crayfish neuromuscular junction studied with fura-2 imaging. Ann N Y Acad Sci 635:452-454.

Delgado R, Maureira C, Oliva C, Kidokoro Y, Labarca P (2000) Size of vesicle pools, rates of mobilization, and recycling at neuromuscular synapses of a Drosophila mutant, shibire. Neuron 28:941-953.

DeMill CM, Delaney KR (2005) Interaction between facilitation and presynaptic inhibition at the crayfish neuromuscular junction. J Exp Biol 208:2135-2145.

Denker A, Bethani I, Kröhnert K, Körber C, Horstmann H, Wilhelm BG, Barysch SV, Kuner T, Neher E, Rizzoli SO (2011a) A small pool of vesicles maintains synaptic activity in vivo. Proc Natl Acad Sci U S A 108:17177-17182.

Denker A, Kröhnert K, Bückers J, Neher E, Rizzoli SO (2011b) The reserve pool of synaptic vesicles acts as a buffer for proteins involved in synaptic vesicle recycling. Proc Natl Acad Sci U S A 108:17183-17188.

Denker A, Kröhnert K, Rizzoli SO (2009) Revisiting synaptic vesicle pool localization in the Drosophila neuromuscular junction. J Physiol 587:2919-2926.

Denker A, Rizzoli SO (2010) Synaptic vesicle pools: an update. Front Synaptic Neurosci 2:135.

Dixon D, Atwood HL (1985) Crayfish motor nerve terminal's response to serotonin examined by intracellular microelectrode. J Neurobiol 16:409-424.

Dixon D, Atwood HL (1989a) Phosphatidylinositol system's role in serotonin-induced facilitation at the crayfish neuromuscular junction. J Neurophysiol 62:239-246.

Dixon D, Atwood HL (1989b) Conjoint action of phosphatidylinositol and adenylate cyclase systems in serotonin-induced facilitation at the crayfish neuromuscular junction. J Neurophysiol 62:1251-1259.

Dudel J (1965) Facilitatory effects of 5-hydroxy-tryptamine on the crayfish neuromuscular junction. Naunyn-Schmiedebergs Arch exp Path Pharm 249:515–528

Dudel J, Kuffler SW (1961a) The quantal nature of transmission and spontaneous miniature potentials at the crayfish neuromuscular junction. J Physiol 155:514-529.

Dudel J, Kuffler SW (1961b) Mechanism of facilitation at the crayfish neuromuscular junction. J Physiol 155:530-542.

Dudel J, Kuffler SW (1961c) Presynaptic inhibition at the crayfish neuromuscular junction. J Physiol 155:543-562.

Edelstein A, Amodaj N, Hoover K, Vale R, Stuurman N (2010) Computer control of microscopes using μManager. Curr Protoc Mol Biol Chapter 14:Unit14.20.

Evans PD, Kravitz EA, Talamo BR (1976) Octopamine release at two points along lobster nerve trunks. J Physiol 262:71-89.

Fischer L, Florey E (1983) Modulation of synaptic transmission and excitation-contraction coupling in the opener muscle of the crayfish, Astacus leptodactylus, by 5-hydroxytryptamine and octopamine. Journal of Experimental Biology 102:187-198.

Florey E, Cahill MA (1982) The innervation pattern of crustacean skeletal muscle. Cell Tissue Res 224:527-541.

Gad H, Löw P, Zotova E, Brodin L, Shupliakov O (1998) Dissociation between Ca2+-triggered synaptic vesicle exocytosis and clathrin-mediated endocytosis at a central synapse. Neuron 21:607-616.

Gaffield MA, Betz WJ (2006) Imaging synaptic vesicle exocytosis and endocytosis with FM dyes. Nat Protoc 1:2916-2121.

Gaffield MA, Rizzoli SO, Betz WJ (2006) Mobility of synaptic vesicles in different pools in resting and stimulated frog motor nerve terminals. Neuron 51:317-325.

Glusman S, Kravitz EA (1982) The action of serotonin on excitatory nerve terminals in lobster nerve-muscle preparations. J Physiol 325:223-241.

Goldfischer S, Kress Y, Coltoff-Schiller B, Berman J (1981) Primary fixation in osmium-potassium ferrocyanide: the staining of glycogen, glycoproteins, elastin, an intranuclear reticular structure, and intercisternal trabeculae. J Histochem Cytochem 29:1105-1111.

Govind CK, Meiss DE (1979) Quantitative comparison of low- and high-output neuromuscular synapses from a motorneuron of the lobster (*Homarus americanus*). Cell Tissue Res 198:455-463.

Graham C, Karnovsky J (1966) The early stages of absorption of injected horseradish peroxidase in the proximal tubules of mouse kidney: ultrastructrual cytochemistry by a new technique. J Histochem Cytochem 14:291-302.

Harata N, Pyle JL, Aravanis AM, Mozhayeva M, Kavalali ET, Tsien RW (2001) Limited numbers of recycling vesicles in small CNS nerve terminals: implications for neural signaling and vesicular cycling. Trends Neurosci 24:637-643.

Harrington CC, Atwood HL (1995) "Satellite cells" and nerve terminals in the crayfish opener muscle visualized with fluorescent dyes. J Comp Neurol 361:441-450.

Harris-Warrick RM, Kravitz EA (1984) Cellular mechanisms for modulation of posture by octopamine and serotonin in the lobster. J Neurosci 4:1976-1993.

Henkel AW, Lübke J, Betz WJ (1996) FM1-43 dye ultrastructural localization in and release from frog motor nerve terminals. Proc Natl Acad Sci U S A 93:1918-1923.

Heuser JE, Reese TS (1973) Evidence for recycling of synaptic vesicle membrane during transmitter release at the frog neuromuscular junction. J Cell Biol 57:315-344.

Heuser JE, Reese TS, Landis DMD (1974) Functional changes in frog neuromuscular junctions studied with freeze-fracture. J Neurocytol 3:109-131.

Holtzman E, Freeman AR, Kashner LA (1971) Stimulation-dependent alterations in peroxidase uptake at lobster neuromuscular junctions. Science (New York, NY) 173:733.

Hong SJ, Lnenicka GA (1997) Characterization of a P-type calcium current in a crayfish motoneuron and its selective modulation by impulse activity. J Neurophysiol 77:76.

Hoopmann P, Rizzoli SO, Betz WJ (2012) Imaging synaptic vesicle recycling by staining and destaining vesicles with FM dyes. Cold Spring Harb Protoc 2012:77-83.

Hosaka M, Hammer RE, Südhof TC (1999) A Phospho-Switch Controls the Dynamic Association of Synapsins with Synaptic Vesicles. Neuron 24:377-387.

Jahn R., Sudhof,T.C. (1994) Synaptic vesicles and exocytosis. Annu. Rev. Neurosci. 17:219-246.

Jahromi SS, Atwood HL (1967) Ultrastructural features of crayfish phasic and tonic muscle fibers. Can J Zool 45:601-606.

Jahromi SS, Atwood HL (1974) Three-dimensional ultrastructure of the crayfish neuromuscular apparatus. J Cell Biol 63:599-613.

Johnstone AF, Viele K, Cooper RL (2011) Structure/function assessment of synapses at motor nerve terminals. Synapse 65:287-299.

Kamin D, Lauterbach MA, Westphal V, Keller J, Schönle A, Hell SW, Rizzoli SO (2010) High- and low-mobility stages in the synaptic vesicle cycle. Biophys J 99:675-684.

Kay AR, Alfonso A, Alford S, Cline HT, Holgado AM, Sakmann B, Snitsarev VA, Stricker TP, Takahashi M, Wu LG (1999) Imaging synaptic activity in intact brain and slices with FM1-43 in C. elegans, lamprey, and rat. Neuron 24:809-817.

Kerkut GA, Leake LD, Shapira A, Cowan S, Walker RJ (1965) The presence of glutamate in the nerve-muscle perfusates of *Helix, Carcinus* and *Periplaneta*. Comp Biochem Physiol 15:485-502.

King MJ, Atwood HL, Govind CK (1996) Structural features of crayfish phasic and tonic neuromuscular terminals. J Comp Neurol 372:618-626.

Kuromi H, Honda A, Kidokoro Y (2004) Ca2+ influx through distinct routes controls exocytosis and endocytosis at drosophila presynaptic terminals. Neuron 41:101-111.

Kuromi H, Kidokoro Y (1998) Two distinct pools of synaptic vesicles in single presynaptic boutons in a temperature-sensitive Drosophila mutant, shibire. Neuron 20:917-925.

Kuromi H, Kidokoro Y (1999) The optically determined size of exo/endo cycling vesicle pool correlates with the quantal content at the neuromuscular junction of Drosophila larvae. J Neurosci 19:1557-1565.

Kuromi H, Kidokoro Y (2000) Tetanic stimulation recruits vesicles from reserve pool via a cAMP-mediated process in Drosophila synapses. Neuron 27:133-143.

Kuromi H, Kidokoro Y (2002) Selective replenishment of two vesicle pools depends on the source of Ca2+ at the Drosophila synapse. Neuron 35:333-343.

Listerman LR, Deskins J, Bradacs H, Cooper RL (2000) Heart rate within male crayfish: social interactions and effects of 5-HT. Comp Biochem Physiol A Mol Integr Physiol 125:251-263.

Livingstone MS, Harris-Warrick RM, Kravitz EA (1980) Serotonin and octopamine produce opposite postures in lobsters. Science 208:76-79.

Livingstone MS, Schaeffer SF, Kravitz EA (1981) Biochemistry and ultrastructure of serotonergic nerve endings in the lobster: Serotonin and octopamine are contained in different nerve endings. Journal of Neurobiology 12:27-54.

Miller M, Heuser E (1984) Endocytosis of synaptic vesicle membrane at the frog neuromuscular junction. J Cell Biol 98:685-698.

Neves G, Lagnado L (1999) The kinetics of exocytosis and endocytosis in the synaptic terminal of goldfish retinal bipolar cells. J Physiol 515:181-202.

Paillart C, Li J, Matthews G, Sterling P (2003) Endocytosis and vesicle recycling at a ribbon synapse. The Journal of neuroscience 23:4092.

Pan B, Zucker RS (2009) A general model of synaptic transmission and short-term plasticity. Neuron 62:539-554.

Reist NE, Buchanan J, Li J, DiAntonio A, Buxton EM, Schwarz TL (1998) Morphologically docked synaptic vesicles are reduced in synaptotagmin mutants of Drosophila. J Neurosci 18:7662-7673.

Richards DA, Bai J, Chapman ER (2005) Two modes of exocytosis at hippocampal synapses revealed by rate of FM1-43 efflux from individual vesicles. J Cell Biol 168:929-939.

Richards DA, Guatimosim C, Betz WJ (2000) Two endocytic recycling routes selectively fill two vesicle pools in frog motor nerve terminals. Neuron 27:551-559.

Richards DA, Guatimosim C, Rizzoli SO, Betz WJ (2003) Synaptic vesicle pools at the frog neuromuscular junction. Neuron 39:529-541.

Rizzoli SO, Betz WJ (2004) The structural organization of the readily releasable pool of synaptic vesicles. Science 303:2037-2039.

Rizzoli SO, Betz WJ (2005) Synaptic vesicle pools. Nat Rev Neurosci 6:57-69.

Robbins J (1959) The excitation and inhibition of crustacean muscle by amino acids. J Physiol 148:39-50.

Roos J, Kelly RB (1999) The endocytic machinery in nerve terminals surrounds sites of exocytosis. Curr Biol 9:1411-1414.

Ryan TA, Reuter H, Wendland B, Schweizer FE, Tsien RW, Smith SJ (1993) The kinetics of synaptic vesicle recycling measured at single presynaptic boutons. Neuron 11:713-724.

Sabatini BL, Regehr WG (1996) Timing of neurotransmission at fast synapses in the mammalian brain. Nature 384:170-172.

Sandell JH, Masland RH (1988) Photoconversion of some fluorescent markers to a diaminobenzidine product. J Histochem Cytochem 36:555-559.

Schikorski T (2014) Readily releasable vesicles recycle at the active zone of hippocampal synapses. Proc Natl Acad Sci U S A 111:5415-5420.

Schikorski T, Stevens CF (2001) Morphological correlates of functionally defined synaptic vesicle populations. Nat Neurosci 4:391-395.

Sherman RG, Atwood HL (1972) Correlated electrophysiological and ultrastructural studies of a crustacean motor unit. J Gen Physiol 59:586-615.

Sihra TS, Wang JK, Gorelick FS, Greengard P (1989) Translocation of synapsin I in response to depolarization of isolated nerve terminals. Proc Natl Acad Sci U S A 86:8108-8112.

Siksou L, Rostaing P, Lechaire JP, Boudier T, Ohtsuka T, Fejtová A, Kao HT, Greengard P, Gundelfinger ED, Triller A, Marty S (2007) Three-dimensional architecture of presynaptic terminal cytomatrix. J Neurosci 27:6868-6877.

Southard RC, Haggard J, Crider ME, Whiteheart SW, Cooper RL (2000) Influence of serotonin on the kinetics of vesicular release. Brain Res 871:16-28.

Staras K, Branco T, Burden JJ, Pozo K, Darcy K, Marra V, Ratnayaka A, Goda Y (2010) A vesicle superpool spans multiple presynaptic terminals in hippocampal neurons. Neuron 66:37-44.

Sun JY, Wu XS, Wu LG (2002) Single and multiple vesicle fusion induce different rates of endocytosis at a central synapse. Nature 417:555-559.

Tabor JN, Cooper RL (2002) Physiologically identified 5-HT2-like receptors at the crayfish neuromuscular junction. Brain Res 932:91-98.

Takei K, Mundigl O, Daniell L, De Camilli P (1996) The synaptic vesicle cycle: a single vesicle budding step involving clathrin and dynamin. J Cell Biol 133:1237-1250.

Teng H, Cole JC, Roberts RL, Wilkinson RS (1999) Endocytic active zones: hot spots for endocytosis in vertebrate neuromuscular terminals. J Neurosci 19:4855-4866.

Teng H, Wilkinson RS (2000) Clathrin-mediated endocytosis near active zones in snake motor boutons. J Neurosci 20:7986-7993.

Thompson CS, Atwood HL (1984) Synaptic strength and horseradish peroxidase uptake in crayfish nerve terminals. J Neurocytol 13:267-280.

Tierney AJ, Greenlaw MA, Dams-O'Connor K, Aig SD, Perna AM (2004) Behavioral effects of serotonin and serotonin agonists in two crayfish species, Procambarus clarkii and Orconectes rusticus. Comparative Biochemistry and Physiology Part A: Molecular & Integrative Physiology 139:495-502.

Tierney AJ, Mangiamele (LA (2001) Effects of serotonin and serotonin analogs on posture and agonistic behavior in crayfish. J Comp Physiol A 187:757-767.

Van Harreveld A (1936) A Physiological Solution for Freshwater Crustaceans. Experimental Biology and Medicine 34:428-432.

Vyshedskiy A, Delaney KR, Lin JW (1998) Neuromodulators enhance transmitter release by two separate mechanisms at the inhibitor of crayfish opener muscle. J Neurosci 18:5160-5169.

Wang C, Zucker RS (1998) Regulation of synaptic vesicle recycling by calcium and serotonin. Neuron 21:155-167.

Watanabe S, Liu Q, Davis MW, Hollopeter G, Thomas N, Jorgensen NB, Jorgensen EM (2013) Ultrafast endocytosis at Caenorhabditis elegans neuromuscular junctions. Elife 2:e00723.

Watanabe S, Trimbuch T, Camacho-Pérez M, Rost BR, Brokowski B, Söhl-Kielczynski B, Felies A, Davis MW, Rosenmund C, Jorgensen EM (2014) Clathrin regenerates synaptic vesicles from endosomes. Nature 515:228-233.

Westphal V, Rizzoli SO, Lauterbach MA, Kamin D, Jahn R, Hell SW (2008) Video-rate far-field optical nanoscopy dissects synaptic vesicle movement. Science 320:246-249.

Wilson DM, Davis WJ (1965) Nerve impulse patterns and reflex control in the motor system of the crayfish claw. J Exp Biol 43:193-210.

Wojtowicz JM, Marin L, Atwood HL (1994) Activity-induced changes in synaptic release sites at the crayfish neuromuscular junction. J Neurosci 14:3688-3703.

Wojtowicz JM, Smith BR, Atwood HL (1991) Activity-Dependent Recruitment of Silent Synapses. Ann N Y Acad Sci 627:169-179.

Wu WH, Cooper RL (2012) The regulation and packaging of synaptic vesicles as related to recruitment within glutamatergic synapses. Neuroscience 225:185-198.

Wu WH, Cooper RL (2013) Physiological separation of vesicle pools in low- and high-output nerve terminals. Neurosci Res 75:275-282.

Wu Y, Yeh FL, Mao F, Chapman ER (2009) Biophysical characterization of styryl dye-membrane interactions. Biophys J 97:101-109.

Yeh SR, Fricke RA, Edwards DH (1996) The effect of social experience on serotonergic modulation of the escape circuit of crayfish. Science 271:366-369.

Zhai RG, Bellen HJ (2004) The architecture of the active zone in the presynaptic nerve terminal. Physiology (Bethesda) 19:262-270.

Appendix A – FM1-43 Photoconversion Protocol

Photoconversion of FM1-43 had not been performed on crayfish synapses prior to my investigations. Below is a detailed protocol of the photoconversion procedure, including solutions and personal comments. The protocol was adapted from Denker et al., 2011a.

CHEMICALS AND SOLUTIONS

FM1-43 Photoconversion

Crayfish saline

Components in mM: 195 NaCl, 5.4 KCl, 13.5 $CaCl_2$, 2.6 $MgCl_2$ and 10 4-[2-Hydroxyethyl]piperazine-1-ethanesulfonic acid (HEPES), titrated to pH 7.3 with NaOH.

FM1-43

Stocks of 1 mM prepared by dissolving dye in crayfish ringer and storing at 4°C. Used at a final dye concentration of 10-15 μM.
Note: stock solutions always used within 2-3 days.

ADVASEP-7

Stocks of 10 mM prepared by dissolving ADV-7 powder in distilled water and storing at 4°C. Stock solutions kept at 4°C for as long as needed. Used at a final concentration of 1 mM.

Phosphate buffered solution (for crayfish)

Modified phosphate buffered solution for crayfish preparations (200 mM stock, pH 7.3). Stock solution stored at 4°C and used at a final concentration of 100 mM.

For 300 mL stock:
(1) measure 1.33 g NaH_2PO_4 + 7.16 g Na_2HPO_4
(2) bring volume to 300 mL → check pH (should be ~ 7.4 – 7.5)
(3) add 240 mM NaCl (4.21 g NaCl)
(4) check pH is ~ 7.3

2.5% Glutaraldehyde

Glutaraldehyde stock diluted in crayfish buffered solution and stored at 4°C.

100 mM Ammonium chloride (NH_4Cl)

NH_4Cl dissolved in crayfish buffered solution, stored at 4°C.

3,3'-diaminobenzidine (DAB)

DAB prepared fresh for every experiment and used at a concentration of 1.5 mg/mL (in crayfish buffered solution). Extra caution should be taken when using DAB (see MSDS before preparing).

TEM Processing

Sodium cacodylate buffer (pH 7.4)

400 mM stock solution to be used at final concentration of 100 mM. Stock diluted with dH_20 to reach 100 mM.

Osmium tetroxide

4% Osmium tetroxide stock solution to be used at a final concentration of 1% (in cacodylate buffered solution and dH_20).

Ethanol - *50, 70, 85, 95, 100%*

Spurr's epoxy resin

Make fresh resin every time.
Caution: the resin components are toxic and all MSDS should be consulted prior to use

METHOD

Sample preparation

1. Prepare crayfish opener NMJ as outlined in Chapter 2 – General Materials and Methods

   Note: Ensure that very little connective tissue remains on the surface of the muscle fibers or else visualizing FM1-43-labeled terminals will be difficult.
   Note: Because the crayfish leg will need to be removed from the prep dish in later steps, I recommend gluing the leg to a small piece of glass (e.g. microscope slide adhered to the base of the petri dish) instead of directly onto the plastic. It is easier to remove the shell from the glass.

FM1-43 Loading

2. Perform FM1-43 loading as described in Chapter 3 – Materials and Methods
    - *Incubate tissue in dye-containing solution for up to 5 min*
    - *Stimulate excitor axon for 3 min at 20 Hz frequency*
    - *Upon cessation of stimulation, allow preparation to rest for 1 min then incubate ADVASEP-7 for 1 min*
    - *Rinse preparation with continuous perfusion of dye-free crayfish saline for desired length of time (depends on the experiment)*
    - ***Check fluorescence before continuing!! Ensure that you have a strong signal from terminals and take note of where the terminals of interest are located (tip: use the main axon branch as a reference point and sketch the terminals locations on paper – report estimated distances in microns)***

Fixation

3. After briefly checking fluorescence, remove preparation dish from microscope stage and place in an ice bucket

4. Fix tissue for 20 min in 2.5% glutaraldehyde (in crayfish buffered solution) on ice

5. Move tissue to a dark box and continue fixing for 20-30 min at room temperature

Washing and Quenching

6. Wash tissue in crayfish buffered solution (5-10 min) at 4°C in the dark

7. Quench glutaraldehyde-induced autofluorescence with NH_4Cl wash (10 min, 4°C, dark)

8. Wash with crayfish buffered solution again (3 x 10 min washes, 4°C, dark)

DAB incubation

Tip: Prior to DAB incubation, I recommend removing the leg from the prep dish (gently scrape a clean razor blade against the glue at the base of the shell). I pinned the leg to a reusable "DAB-designated" plastic petri dish that had a shallow layer of sylgard at the bottom. This allowed me to limit the number of materials exposed to DAB.

9. Incubate tissue in freshly made 1.5 mg/mL DAB solution for 35-40 min (4°C, dark)

10. Refresh DAB solution after first incubation and transfer tissue back to microscope stage

Photoconversion (illumination)

11. Find previous terminals of interest using a low power of excitation light
    For this step I used the 75W Xe-lamp (ex. 475 nm)

12. Close the objective aperture/diaphragm until area of illumination (AOI) is ~100 μm in diameter. Adjust the prep so that the AOI is ~100 μm away from the terminals of interest
    There are two reasons why I illuminated an area adjacent to my terminals. First, I wanted to create a fiducial marker (by staining the tissue) for later identification of the terminals. Second, I found that direct illumination of the labeled terminals caused too much photo-damage at the ultrastructural level.
    This step in the photoconversion process could be improved.
    Note: The AOI should be located on the same muscle fiber as the terminals to make the EM steps as easy as possible. However, if the terminals are clustered across more than one fiber, you may not be able to restrict your AOI to just one. In this case, micro-dissection might be more difficult.

13. Switch to a higher power light source (e.g. I used a 120-W X-Cite light). Illuminate area for ~ 20 min at high power
    Check that the surface of the muscle fiber in your AOI is darkening. This AOI will become the fiducial marker. You need to be able to see the dark spot on your muscle to find the terminals later! Draw the location of the darkened AOI on your sketch – estimate distances.

Washing and fixation

14. After illumination, remove the prep from the stage and wash with cold crayfish buffered solution for at least 5 min (4°C)

15. Place tissue into glass vials containing 2.5% glutaraldehyde and keep at 4°C until TEM tissue processing (fix at least overnight)

PROCEED WITH TEM PROCESSING ONCE YOU HAVE A GROUP OF SAMPLES
Do not process single legs – it is not a good use of time or materials

TEM tissue dissection – to be done in MSB 250 (PCN Lab)

16. For each sample/leg, locate the darkened AOI. Determine the location of the terminals using the AOI and your sketches

17. Carefully remove the entire opener muscle as a unit from the shell

Cut the central tendon at the distal end of the propodite segment and gently pull the muscle out, cutting additional tethers in the process. Keep your eyes on the AOI and don't let the fibers separate

18. Isolate and cut your AOI and terminals
    Take note of the approximate length of tissue. In order to differentiate the AOI end from the terminal end after osmication, make one cut straight and the other cut angled (add the cuts to your sketch for later reference)

19. Gently move the cut tissue into a **pre-labeled** small glass vial containing buffered solution
    Tip: use a micropipetter to move the tissue and cut the plastic pipette tip to make the hole bigger for tissue to pass through.
    Coat the inside of the pipette tip with albumin to prevent the tissue from sticking to the plastic pipette tip – once tissue sticks it is gone forever

20. Continue micro-dissecting all samples, placing the dissected tissue into appropriately labeled vials. Record the number of samples per vial.

TEM tissue processing

21. Using a thin-tipped plastic pipette, remove as much buffered solution from the glass vials as possible *without disturbing the tissue*
    The tissue is difficult to see at this step so work carefully.
    Tip: keep the vials positioned at a slight angle so that tissue pools in a bottom corner

22. In the fume hood, make a fresh solution of 1% osmium tetroxide (in 100 mM cacodylate buffer) using proper mixing vials. Add enough osmium solution to cover the tissue (~ 1 mL) and post-fix for ~ 15 min

23. Remove osmium from glass vials and wash samples carefully with distilled water (at least twice)
    Samples will be easier to see at this stage because the osmication will have stained the tissue dark. Now is a good time to count your tissue samples to make sure you haven't lost any.
    Note: it will be impossible to see your AOI because everything is dark… hence the angled cuts coming in handy.

24. Dehydrate tissue with ascending ethanol series
    50, 70, 85, 95 and 100% ethanol – 10 min each
    Do 100% ethanol twice
    Do not allow any water to enter tissue at 100%

Infiltrating, embedding and polymerizing

25. Make fresh Spurr's epoxy resin according to instructions on the box (located under fume hood)

26. Immerse tissue in a 50:50 mixture of Spurr's resin and 100% ethanol for 1 hour to begin infiltration.
    Use a small volume of the 50:50 mixture and continuously rotate the vials so that the tissue remains suspended in the mixture. Monitor the tissue to make sure it does not sink to the bottom of the vials – resin will not infiltrate as well if this occurs

27. Replace the 50:50 mixture with pure resin and allow tissue to infiltrate overnight (rotating)

28. Next day: Embedding
    I. Replace resin and rotate for 4 more hours
    II. During the 4 hours: fill flat, rubber embedding molds half-full with resin and polymerize the molds for 3.5 hours at 70°C
    III. Make labels for molds – see below for template (date, tissue type, length of osmication)
    IV. After 3.5 hours: remove molds from oven, place labels at one end of the molds and fill the remaining volume with fresh resin. Use EM tools to place tissue in the molds. Ensure that the tissue is arranged properly before placing the molds back in the oven.
        If each mold contains multiple fibers, be sure to align them as close together as possible to reduce the area of your block face
        Sketch the blocks in your notebook. Include the label and be sure to identify the individual fibers if there is more than one type

    V. Polymerize molds overnight at 70°C

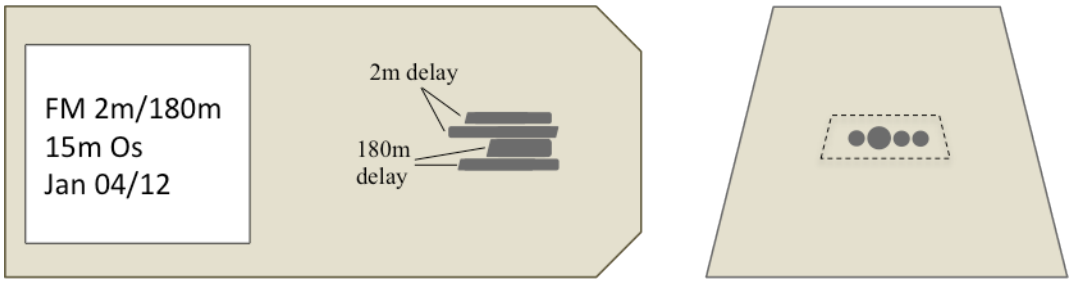

Left: Top view of resin block. Tissue is tightly arranged in parallel on the right end of the block. Labels containing tissue description, length of osmication, and date are on the left end of the block. Be sure to label the individual fibers/bundles on paper sketches (as shown above).
Right: Block face view. The tissue is clustered in the center of the block. When terminals of interest are found, the block face is trimmed (dotted line) to reduce surrounding resin and allow more sections per grid.

Tissue sectioning & looking for labeled terminals

29. Take the molds out of the oven and remove the polymerized blocks. *While the blocks are still warm from the oven*, trim excess resin around the tissue using a razor blade

    The tissue is easiest to trim when it's still relatively soft from the oven. Additionally, trimming with a razor blade saves a LOT of time sectioning with a glass knife. Get as close to the tissue on the block face as you can without cutting the tissue.

30. After trimming with a razor blade, continue trimming the block face using the ultramicrotome and a glass knife. Trim until you reach tissue.

31. Finding terminals of interest:

    This part of the protocol is intuitive. You will need to have an understanding of where the terminals of interest are located along the fibers and how many microns you will need to cut to reach them. My strategy was to cut a certain distance into the block (20 – 50 μm) with a glass knife and then sample the terminals by cutting a small number of thin sections (cut at 60 – 80 nm) with a diamond knife. I would collect those sections on a 200-Hex copper grid and view them on the transmission electron microscope. If I could not see labeled vesicles I would return to the lab, cut another 20-50 μm into the block and sample again. I repeated this procedure until I found terminals with black vesicles or until the tissue ran out. This strategy is imperfect because terminals of interest can be missed during the thick sectioning. However, I found it impossible to tell whether I was in a good region using light microscopy and sectioning the entire block was too time consuming.

    <u>This is the second step in the photoconversion process that could use improvement.</u>

32. Once a region of interest is found, trim the sides of the block face as narrow as possible and cut a continuous series of sections (set the ultramicrotome to cut at 60 nm). Collect the series on freshly made 1% parlodion-coated slotted grids.

Imaging

33. View the series on the TEM (JEOL 1400) and take images of the regions of interest for analysis

    I took images at 40,000x magnification

34. Calibrate images by imaging a carbon replica grid (0.463 μm spacing) at the same magnifications

Appendix B – Horseradish Peroxidase and Cationized Ferritin Loading and TEM

Attempts were also made to use horseradish peroxidase (HRP) and cationized ferritin (CF) as tracers for recycling vesicles. These tracers were utilized because they provided a means to label recycling structures without the drudgery of the photoconversion procedure. As with FM1-43, both HRP and CF do not fully penetrate cell membranes and will remain inside membrane-bound compartments following endocytosis (Graham and Karnovsky, 1966; Paillart et al., 2003).

HRP is a 44 kDa protein which oxidizes DAB in the presence of the oxidizing agent hydrogen peroxide (Graham and Karnovsky, 1966). This reaction does not require photo-illumination, which was a challenging step in the FM1-43 photoconversion procedure. HRP has been previously used to label synaptic vesicles in crustacean motor neurons (Holtzman et al., 1971; Thompson and Atwood, 1984) while photoconverted FM1-43 had not.

Cationized ferritin is an electron dense tracer prepared by coupling horse spleen ferritin with *N, N* Dimethyl-1,3propanediamine (DMPA) via carbodiimide activation of the protein carboxyl groups (Danon et al., 1972). The polycationic derivative of ferritin interacts with the negative charges on cell surfaces, making it a suitable tracer for endocytosed membrane compartments. CF has been utilized as a tracer for synaptic vesicles and other endocytic compartments in presynaptic terminals of the retina (Paillart et al., 2003) and cultured hippocampal neurons (Watanabe et al., 2013), but not crayfish synapses. CF was an ideal tracer due to its inherent electron density. It appeared to provide an even simpler strategy for vesicle labeling compared to oxidization of DAB with both the FM1-43 and HRP protocols.

Horseradish peroxidase labeling protocol

HRP loading, fixation, and washing

The HRP loading protocol was adapted from Thompson and Atwood (1984). HRP in crayfish saline was bath-applied at a final concentration of 1-2% for 15-60 min prior to loading to give the tracer time to reach the synaptic clefts. A small wax dam was built around the exposed opener muscle to reduce the volume of HRP solution bathing the tissue. HRP was loaded with 20-Hz axon stimulation for various lengths of time (3-20 min). After loading, the preparations were allowed to rest for various lengths of time (5-10 min) before being fixed with 2.5% glutaraldehyde in crayfish buffered solution. The tissue was kept in fixative overnight at 4°C and dissected the following day in buffered solution. The dissected muscles were then incubated for 15 minutes in the dark at room temperature with 0.03% DAB solution. Following incubation the muscles were immersed in a 0.03% DAB and 0.01% H_2O_2 buffered solution for 30 minutes in the dark at room temperature. After the DAB reaction the muscles were placed back in fixative and stored until TEM processing.

TEM tissue processing

All preparations were micro-dissected in crayfish buffered solution to isolate single or small bundles of muscle fibers containing the terminals of interest. The dissected tissue was post-fixed in 1% osmium tetroxide and 1% potassium ferrocyanide in cacodylate buffer for 15 minutes and then washed in distilled water. The tissue was washed in distilled water and dehydrated in an ascending ethanol series (50, 70, 85, 95, 100% two times), immersed in a 50:50 mixture of Spurr's epoxy resin and 100% ethanol for 1 hour, and then in pure resin overnight. The tissue was embedded the next day and polymerized at 70°C overnight.

Tissue sectioning and imaging

For TEM, tissue blocks were trimmed and thin-sectioned (60-90 nm, or silver interference colour) using a 45° DiATOME diamond knife. Sections were examined with a JEOL 1400 transmission electron microscope and imaged with a Gatan SC1000 digital camera.

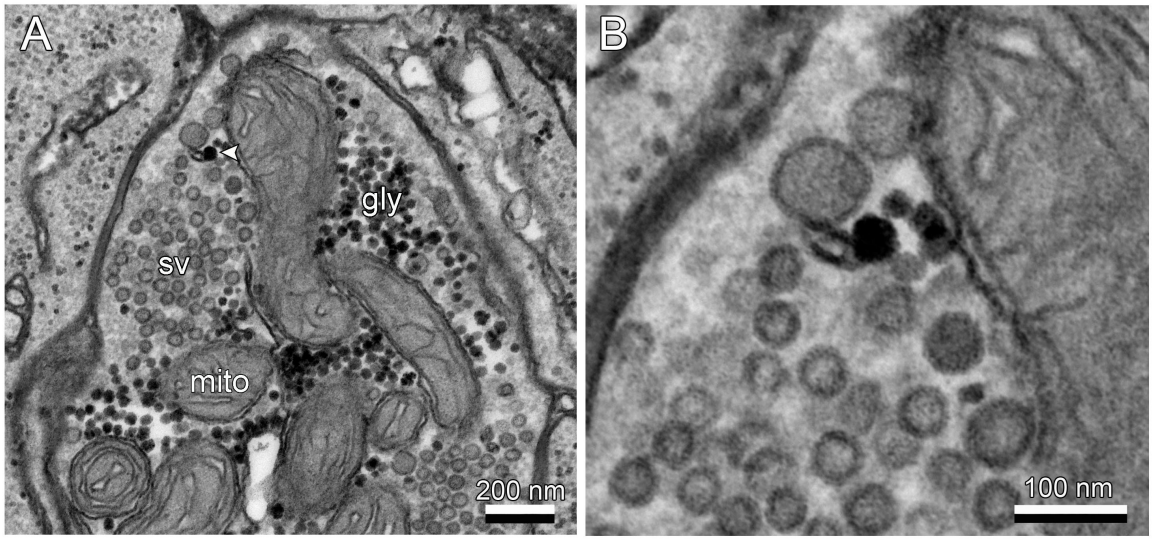

Figure 20. HRP labeling is sparse in crayfish terminals. (A) Terminals loaded with bath-applied 1-2% HRP solution showed a small fraction of HRP-containing vesicles (arrowhead), making quantitation of labeled vesicles difficult. The putative HRP-labeled vesicles were also similar to stained glycogen rosettes in both lumenal density and size at x80,000 magnification. (B) The distinction is more apparent between labeled vesicles and stained glycogen when viewed at higher magnification. Mito: mitochondria, sv: synaptic vesicles, gly: glycogen.

Cationized ferritin labeling protocol

CF loading, fixation, and washing

Because CF had not previously been used as a tracer for recycling vesicles in crayfish tissue, both the concentration and the incubation time needed to be determined.

The incubation time needed to allow for a sufficient amount of the tracer to diffuse into the synaptic clefts. Stock CF (10 mg/ml) was diluted 1:40, 1:10, 1:5 and 1:2 in crayfish saline and bath-applied from 1-20 minutes before loading. The incubation did not extend beyond 20 minutes because CF was reported to have detrimental effects when applied for too long. The tracer was loaded with 20-Hz axonal stimulation for different lengths of time. Following stimulation, preparations were washed in normal saline and fixed at 4°C until they were processed for TEM.

TEM tissue processing, sectioning and imaging

Tissue was processed, sectioned and imaged with the same procedures as the photoconverted FM1-43 tissue (Chapter 4).

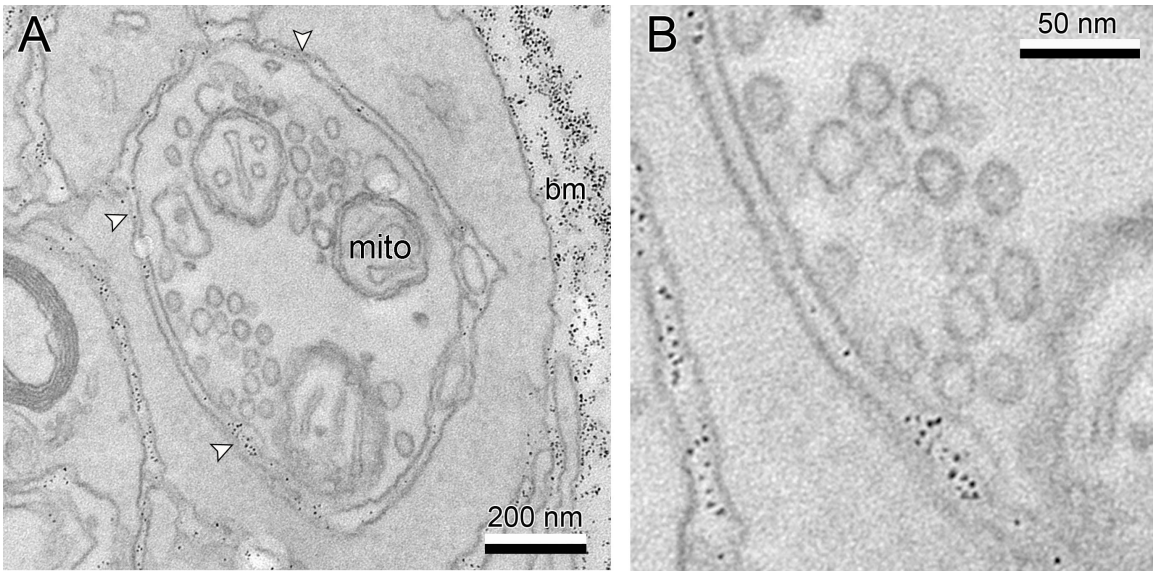

Figure 21. Cationized ferritin does not label synaptic vesicles in crayfish terminals. (A) Terminals loaded with bath-applied 2 mg/mL CF solution showed almost no evidence of the tracer inside synaptic vesicles. The majority of the tracer was trapped in the basement membrane so only a fraction moved into the synaptic cleft (B). The crayfish NMJ is not a suitable preparation for ferritin labeling because there is too much tissue between the external ferritin solution and synaptic cleft. X100,000. mito: mitochondrion, bm: basement membrane.

Note on glycogen staining

The first tissue samples that were processed for TEM showed dark staining of glycogen (Figure 22A). This posed a problem for experimental analyses because the stained glycogen rosettes resembled the dense, labeled synaptic vesicles. In order to ensure that glycogen would not be confused for labeled vesicles, potassium ferrocyanide was eliminated from the osmium tetroxide solution (Goldfischer et al., 1981). Tissue that was processed in the absence of potassium ferrocyanide did not have densely stained glycogen (Figure 22B). Instead, the glycogen appeared as a light "fuzz" in the center of imaged terminals and was easily distinguished from labeled vesicles.

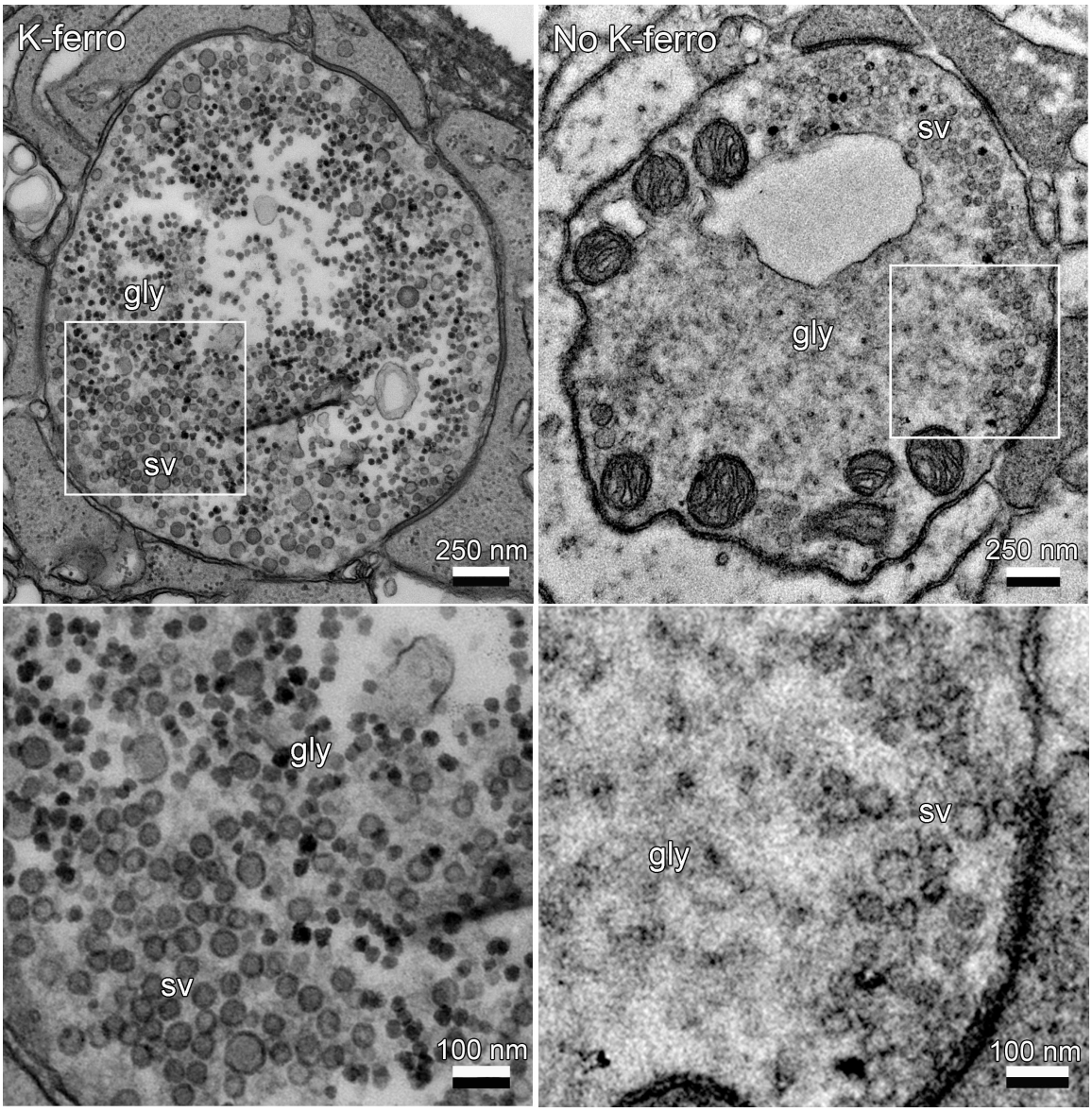

Figure 22. Potassium ferrocyanide enhances the staining of glycogen. (Top left, bottom left) When potassium ferrocyanide is combined with osmium tetroxide it produces enhanced contrast-staining of glycogen. Stained glycogen obscures the identification of vesicles containing photoconverted FM1-43 or HRP because both have even electron density. (Top right, bottom right) When osmium tetroxide is applied without potassium ferrocyanide, glycogen has poor contrast and does not interfere with the identification of synaptic vesicles.